Journal of Advanced Research 34 (2021) 93–107

Contents lists available at ScienceDirect

Journal of Advanced Research

journal homepage: www.elsevier.com/locate/jare

Neomenthol prevents the proliferation of skin cancer cells by restraining tubulin polymerization and hyaluronidase activity

Kaneez Fatima [a,b], Nusrat Masood [a], Zahoor Ahmad Wani [a], Abha Meena [a,b], Suaib Luqman [a,b,*]

[a] Bioprospection and Product Development Division, CSIR-Central Institute of Medicinal and Aromatic Plants, Lucknow 226015, Uttar Pradesh, India
[b] Academy of Scientific and Innovative Research (AcSIR), Ghaziabad 201002, Uttar Pradesh, India

GRAPHICAL ABSTRACT

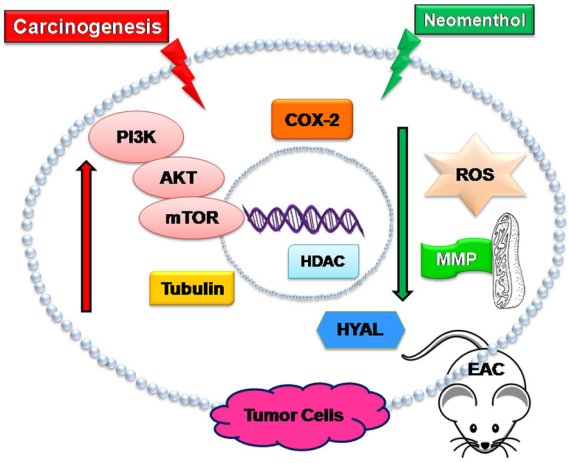

Abbreviations: AKLP, Alkaline phosphatase; AA, Arachidonic acid; Ab/Am, Antibiotic/antimycotic; BE, Binding energy; BIL, Bilirubin total & direct; BSA, Bovine serum albumin; BUN, Blood urea nitrogen; CATD, Cathepsin D; COX-2, Cyclooxygenase 2; DFMO, α-difluoro methyl ornithine; DOXO, Doxorubicin; CM-H2DCFDA, Chloromethyl derivative of dichloro fluorescin diacetate; CHOL, Cholesterol; CRTN, Creatinine; DMEM, Dulbecco's minimal essential media; DHFR, Dihydrofolatereductase; DCFDA, 2′,7′ dichloro fluorescin diacetate; DNA, Deoxyribonucleic acid; DMSO, Dimethyl sulfoxide; ELISA, enzyme-linked immunosorbent assay; EC_{50}, Half maximal effective concentration; EDTA, Ethylene diamine tetra acetic acid; EAC, Ehlrich Ascites Carcinoma; FBS, Fetal bovine serum; FOX, Ferrous oxidation-xylenol orange; FACS, Fluorescence-Activated Cell Sorting; FDA, Food and Drug Administration; GAPDH, Glyceraldehyde 3-phosphate dehydrogenase, HEPES, N-2-hydroxyethylpiperazine-N′-2-ethanesulfonic acid; HYAL, Hyaluronidase; HA, Hyaluronic acid; HDL, High density lipoprotein; HDAC, Histone deacetylase; IC_{50}, Half maximal inhibitory concentration; IDT, Integrated DNA Technologies; Ki, Inhibitory constant; LOX-5, Lipoxygenase-5; LDH, Lactate dehydrogenase; MTT, 3-(4,5-dimethylthiazol-2-yl)-2,5-diphenyltetrazolium bromide; MTX, Methotrexate; mTOR, Mammalian target of rapamycin; MEF, Mean erythrocyte fragility; NAC, N-acetyl cysteine; MMP, Mitochondrial membrane potential; NADPH, Nicotinamide adenine dinucleotide phosphate hydrogen; NRU, Neutral red uptake; NaOH, Sodium hydroxide; ODC, Ornithine decarboxylase; OF, Osmotic fragility; OECD, Organization for Economic Co-operation and Development; PEP A, pepstatin A; PI3K, Phosphotidyl inositol-3 kinase; PDT, Podophyllotoxin; PKB/Akt, Protein kinase B; PI, Propidium iodide; PDB, Protein Data Bank; PCR, Polymerase chain reaction; PBS, Phosphate buffer saline; RPMI, Roswell park memorial institute; ROS, Reactive oxygen species; RNA, Ribonucleic acid; RNase A, Ribonuclease A; Rh123, Rhodamine 123; RIPA, Radio immune precipitation assay buffer; RBC, Red blood cell; SRB, Sulphorhodamine B; SGOT, Aspartate aminotransferase; SGPT, Alanine aminotransferase; TPA, 12-*O*-Tetradecanoylphorbol-13-acetate; TCA, Tricarboxylic acid; TPR, Total protein; TRIG, Triglyceraldehyde; TRPM8, Transient receptor potential member 8; TMPD, N,N,N′,N′-tetramethyl-p-phenylenediamine; TNBS, Trinitrobenzenesulphonic acid; URIC, Uric acid; WBC, White blood cell.

Peer review under responsibility of Cairo University.

* Corresponding author at: Bioprospection and Product Development Division, CSIR-Central Institute of Medicinal and Aromatic Plants, Lucknow 226015, Uttar Pradesh, India.

E-mail address: s.luqman@cimap.res.in (S. Luqman).

https://doi.org/10.1016/j.jare.2021.06.003

ARTICLE INFO

Article history:
Received 12 September 2020
Revised 7 June 2021
Accepted 7 June 2021
Available online 10 June 2021

Keywords:
Neomenthol
Hyaluronidase
Human epidermoid carcinoma
Ehrlich Ascites Carcinoma
Tubulin
Cancer biomarker

ABSTRACT

Introduction: Neomenthol, a cyclic monoterpenoid, is a stereoisomer of menthol present in the essential oil of *Mentha* spp. It is used in food as a flavoring agent, in cosmetics and medicines because of its cooling effects. However, neomenthol has not been much explored for its anticancer potential. Additionally, targeting hyaluronidase, Cathepsin-D, and ODC by phytochemicals is amongst the efficient approach for cancer prevention and/or treatment.

Objectives: To investigate the molecular and cell target-based antiproliferative potential of neomenthol on human cancer (A431, PC-3, K562, A549, FaDu, MDA-MB-231, COLO-205, MCF-7, and WRL-68) and normal (HEK-293) cell lines.

Methods: The potency of neomenthol was evaluated on human cancer and normal cell line using SRB, NRU and MTT assays. The molecular target based study of neomenthol was carried out in cell-free and cell-based test systems. Further, the potency of neomenthol was confirmed by quantitative real-time PCR analysis and molecular docking studies. The *in vivo* anticancer potential of neomenthol was performed on mice EAC model and the toxicity examination was accomplished through *in silico*, *ex vivo* and *in vivo* approaches.

Results: Neomenthol exhibits a promising activity (IC_{50} 17.3 ± 6.49 μM) against human epidermoid carcinoma (A431) cells by arresting the G2/M phase and increasing the number of sub-diploid cells. It significantly inhibits hyaluronidase activity (IC_{50} 12.81 ± 0.01 μM) and affects the tubulin polymerization. The expression analysis and molecular docking studies support the *in vitro* molecular and cell target based results. Neomenthol prevents EAC tumor formation by 58.84% and inhibits hyaluronidase activity up to 10% at 75 mg/kg bw, *i.p.* dose. The oral dose of 1000 mg/kg bw was found safe in acute oral toxicity studies.

Conclusion: Neomenthol delayed the growth of skin carcinoma cells by inhibiting the tubulin polymerization and hyaluronidase activity, which are responsible for tumor growth, metastasis, and angiogenesis.

Introduction

Natural products are used by humans since ancient times and play a significant role in the treatment of various diseases, including cancer. About 50–60% of anticancer drugs are either obtained from natural products or based on the scaffold resembling natural products [1]. Even though many anticancer drugs are available, the treatment of cancer is still a challenge due to chemo-resistance, efficacy, and off-target effect. Hence, there is a constant need to explore the plants for novel phytochemicals with high selectivity, efficacy and reduces the toxicity. Neomenthol is a cyclic monoterpenoid and a stereoisomer of menthol that has not been explored much for anticancer activities but possesses cooling-soothing effects like menthol as well as the medicinal assets [2]. Majorly, neomenthol and menthol are present in *Mentha arvensis* and *Mentha piperita* essential oils. The neomenthol is the most stable stereoisomer of menthol, shows higher stability than other stereoisomers such as isomenthol, neo-isomenthol. It is used in food as a flavoring agent and in cosmetics/medicines because of its cooling effects. The cooling sensation observed after mint oil application on the skin is because of the binding of both menthol and neomenthol with the TRPM8 receptors localized on skin cells [3,4]. Owing to its cooling action, it is widely used in a range of medicines treating sore throats and mouth irritations. It is also used for the treatment of minor aches and sprains, and in nasal decongestants. Menthol is also added to various oral hygiene products, including toothpaste, mouthwashes, and chewing gums [5]. Besides therapeutic and cosmeceutical usage, reports suggest that menthol possesses anticancer potential [6,7], however, reports on neomenthol as an anticancer agent are still in an elusive stage.

The modulation of cancer biomarkers (prognostic, predictive, and diagnostic) using phytochemicals is considered amongst the promising approaches to sustain homeostasis. It does so by regulating the deregulated signaling pathways in cancer cells. Many reports suggest the anticancer potential of terpenoids, which targets various prognostic/diagnostic biomarkers and modulates signal transduction pathways in cancer [6–8]. It is also revealed that monoterpenes can prevent *in vivo* tumor growth in a variety of organ systems in animal models, including skin [9], breast [10], lung [11], and liver [12]. Considering the wide application of terpenoids in targeting cancer biomarkers, the present study aims to explore the antiproliferative as well as molecular and cell target based effect of neomenthol on various prognostic biomarkers involved in initiation (tubulin, PI3K, PKB, mTOR), promotion (COX-2, LOX-5, and HDAC) and progression (DHFR, hyaluronidase, ODC, Cathepsin D) stages of cancer. Moreover, the concentration-dependent efficacy of neomenthol was also evaluated in a cell-free system and cell-based target/biomarkers. The potency of neomenthol was confirmed by studying the expression analysis of the targeted gene/enzymes and molecular docking studies with the receptor/protein. Further, the *in vitro* results were confirmed in an EAC model of mice besides safety and toxicity examination.

Material and methods

Chemicals

All the chemicals and reagents used for the experiments were of analytical grade. DMSO, isopropanol, formaldehyde were from E-Merck Ltd, Mumbai, India. DMEM and FBS were procured from Gibco, Thermo Fisher Scientific India Pvt. Ltd., Mumbai, India. (+)-Neomenthol (98.5%), MTT, NRU and SRB dyes, propidium iodide, RNase A, DCF-DA, rhodamine123, trizol, antibiotic–antimycotic (Ab/Am) solution, trypsin, phosphate-buffered saline (PBS), hemoglobin, ornithine decarboxylase, cathepsin D, dihyro folate reductase, hyaluronidase, hyaluronic acid, MTX, pepstatin A, DFMO, NAC, celecoxib, zileuton, and sodium/potassium phosphate were purchased from Sigma-Aldrich, Bengaluru, India.

Lipoxygenase, cycloxygenase were purchased from Cayman Chemical Company, Ann Arbor, Michigan, USA. Sodium bicarbonate and trichloroacetic acid were obtained from Himedia Ltd, Mumbai, India.

Antiproliferative activity evaluation by SRB, NRU, and MTT assays

The antiproliferative potential of neomenthol was analyzed by performing SRB, NRU, and MTT assays using organ-specific human cancer cell lines: MDA-MB-231 (breast ER-ve adenocarcinoma), K-562 (erythroid leukemia), WRL-68 (hepatocellular carcinoma), PC-3 (prostate carcinoma), COLO-205 (colon carcinoma), MCF-7 (breast ER + ve adenocarcinoma), A431 (skin carcinoma), A549 (lung carcinoma), FaDu (hypo-pharyngeal carcinoma) and HEK-293 (embryonic kidney cell line). These cell lines were either procured from the National Centre for Cell Sciences (NCCS), Pune, India or acquired from CSIR-Central Drug Research Institute, Lucknow, India, and cultured in respective media supplemented with 1% Ab/Am solution and 10% FBS (pH 7.2–7.4) and incubated in a CO_2 incubator at 37 °C temperature, 95% humidity.

The 3-(4, 5-dimethylthiazol-2-yl)-2, 5-diphenyltetrazolium bromide (MTT) assay was carried out by following the method described by Mosmann [13]. After attaining 80–90% confluency, the cells were trypsinized and seeded in 96 well plates (approximately 2×10^3 cells/well) followed by the treatment with different concentrations (1 nM, 10 nM, 100 nM, 1 μM, 10 μM, and 100 μM) of neomenthol for 24 h. The MTT dye (500 μg/ml) was added and the formazan crystals were dissolved in DMSO after 4 h of incubation followed by the recording of absorbance at 570 nm using Multiskan™ Go SkanIt Software (4.0 version, Thermo Fisher Scientific, Waltham, MA, USA). The results were expressed as percent cytotoxicity, which was calculated concerning the proliferation of control cells. The neutral red uptake (NRU) assay was performed by following the protocol described by Babich and Borenfreund [14]. Similar to the MTT assay, NRU dye was added in the treated and control cells, and after 3 h of incubation, absorbance was recorded at 540 nm. The results were expressed in terms of percent cytotoxicity, which was calculated concerning the proliferation of control cells. The Sulphorhodamine B (SRB) assay was performed by following the protocol of Skehan [15]. Like MTT and NRU assay, the SRB results were also calculated in terms of percent cytotoxicity. The standard drugs used for three different antiproliferative assays were specific to cell lines i.e., tamoxifen was used against MCF-7, doxorubicin was used against MDA-MB-231, PC-3, A431, taxol was used for A549, and podophyllotoxin was used against COLO-205, K562, FaDu, WRL-68, and HEK-293.

Cell lysate preparation, cell-free, and cell-based enzyme assays

The respective cell lines were treated with neomenthol (100 nM, 1 μM, 10 μM, and 100 μM) for 24 h in 6 well plates followed by the removal of media and lysis by RIPA buffer to extract crude protein. The protein was estimated by two methods, i.e., the Bradford method (1976) and nanodrop, before being used for the enzyme assays. The assays were performed by following two different protocols, the desired enzymes were used in the cell-free test system, and the crude proteins of cells (10 μg) were used for the cell-based assay system.

Cyclooxygenase-2 (COX-2) and Lipoxygenase-5 (LOX-5) assay

The activity of COX-2 was measured according to the method of Kulmacz and Lands [16]. The assay mixture consists of Tris-HCl buffer (100 mM, pH 8.0), hematin (15 μM), EDTA (3 μM), enzyme (100 μg, human recombinant COX-2, Cat No. 60122) or cell lysate (~10 μg protein) and neomenthol/inhibitor (celecoxib). The mixture was pre-incubated at 25 °C for 15 min. Then, the reaction was initiated by the addition of arachidonic acid (AA) and TMPD in the total volume of 200 μL in 96 well plates. The reaction mixture was immediately auto mixed, and the kinetic study was performed at 590 nm for 5 min. The percent inhibition of enzyme activity of neomenthol/inhibitor was plotted concerning the control (non-treated) cells.

The cell lysates or the enzyme (human recombinant LOX-5, Cat No. 60402) was pre-incubated with neomenthol or zileuton (a specific LOX-5 inhibitor). The reaction was initiated by the addition of 40 μM arachidonic acid and kept for 4 min at room temperature. The assay was terminated by the addition of reagent 1 [(4.5 mM $FeSO_4$ in HCl) and reagent 2 (3% NH_4SCN)] and the absorbance was recorded at 480 nm [17]. The percent inhibition of enzyme activity of neomenthol/inhibitor was plotted concerning the control (non-treated) cells.

Dihydrofolate reductase (DHFR) and hyaluronidase (HYAL) assay

Varying concentration of neomenthol/inhibitor (methotrexate) was incubated in the reaction cocktail containing 20 mU/mL DHFR (Cat. No. D6566) or ~10 μg of cell lysate. In contrast, another set was incubated in the reaction cocktail containing 0.1% BSA solution. The experiment was performed in Costar UV 96 well plate. After the addition of the enzyme, the reaction cocktail was immediately mixed after the addition of enzyme/crude protein, and the kinetic study was performed at 340 nm for 5 min. The activity of the enzyme was calculated as Units/mL, according to Hillcoat [18], and the results are presented as percent inhibition, which was calculated concerning control.

The assay was performed by following the protocol described by Dorfman and Ott [19]. Different concentration of neomenthol/inhibitor (N-acetyl cysteine) were incubated in enzyme diluent buffer [20 mM Sodium Phosphate, 77 mM Sodium Chloride, 0.01% Albumin, Bovine, pH 7.0 at 37 °C] containing 4 U/mL enzyme (Cat. No. H3631) /cell lysate (10 μg). The substrate, hyaluronic acid, was added to the mixture and incubated for 45 min. Then, 25 μL of the reaction mixture were pipetted in the plate followed by the addition of 125 μL diluent buffer [24 mM Sodium Acetate, 79 mM Acetic Acid, 0.1% Albumin, Bovine, pH 3.75]. The cocktail was left for 10 min, and the absorbance was recorded at 600 nm. The activity of the enzyme was calculated as Units/mL, and the results are presented as percent inhibition, which was calculated concerning control

Ornithine decarboxylase (ODC) and Cathepsin D (CATD) activity

The ODC activity was analyzed by the modified protocol published by our group earlier [20]. Different concentrations of neomenthol/inhibitor (α-difluoro methyl ornithine) were taken and mixed with a reaction cocktail, followed by the addition of ODC (5 mg/mL, Cat. No. 06503) / cell lysate (10 μg). The addition of perchloric acid terminated the reaction, and the supernatant was further mixed with NaOH, followed by centrifugation and addition of 1-pentanol. The upper organic phase was transferred to a fresh tube containing sodium borate, TNBS, and DMSO. The centrifugation collected the resultant supernatant and the enzyme activity was measured by recording the absorbance at 412 nm. The action of the enzyme was calculated as μM of putrescine per milligram of protein, and the results are presented as percent enzyme inhibition, which was calculated concerning control.

The activity of CATD was measured by following the stop rate determination method [21] using hemoglobin as a substrate. In brief, 5 μL of CATD (Cat. No. C8696) or cell lysate (10 μg) was incubated with neomenthol with or without Pepstatin A (inhibitor), followed by the termination of the reaction by the addition of TCA.

The reaction mixture was centrifuged, and the absorbance of the supernatant was recorded at 280 nm. The specific activity of the enzyme was calculated as described by Smith and Turk [22].

Molecular docking studies and Real-time expression analysis

The molecular interaction of the ligand with the receptor (protein/enzyme) was performed using the software developed by The Scripps Research Institute (Auto-Dock 1.5.4) according to the procedure described by Morris [23]. The Chimera viewer was used to visualize the protein–ligand interacting site, and the hydrophobic interactions are shown by Ligplot software [24].

The RNA was isolated from the treated and non-treated cells using Trizol reagent. 1–3 μg of RNA was used to synthesize cDNA using the High-Capacity cDNA Reverse Transcription Kit [Applied Biosystems™, USA]. The target gene sequences were taken in FASTA format from NCBI, followed by the designing of the primers from the selected forward and reverse sequences using Primer Express® Software v3.0. After designing and confirmation, the primers were synthesized from Integrated DNA Technologies, Inc. (IDT, *Supplementary Table 1*). After cDNA synthesis, the reaction mixture was prepared to contain 2 μL template cDNA, 2.5 μL (10X) buffer, 0.5 μL DNA polymerase, 1 μL (10 mM) dNTPs, 1 μL forward primer, 1 μL reverse primer, 2 μL deionized water to make up the volume to 10 μL/well in 384-well plate. The GAPDH (Glyceraldehyde 3-phosphate dehydrogenase) was used as the internal control, and a non-treated control was also exercised. The real-time assay was performed on a Real-time PCR machine; the "cycle threshold" (C_T) values obtained were used for presenting the relative changes in the gene expression. The relative gene expression was calculated and compared for the treated samples concerning non-treated samples [25].

Cell cycle analysis and tubulin polymerization assay

The cell cycle analysis was carried out following the method described by Singh [26]. The treated and non-treated cells were fixed using 70% ethanol. Before the analysis start, cells were washed, and the pellet was dissolved in propidium iodide staining solution containing RNase A. Then samples were run on a flow cytometer using FACS Diva software. The tubulin polymerization experiment was carried out as per the reported protocol described in the assay kit (BK006P, Cytoskeleton, USA) with slight modification. In brief, tubulin protein (3 mg/mL) was incubated with tubulin polymerization buffer in pre-warmed 96-well microtiter plates at 37 °C in the presence of different concentrations of neomenthol/inhibitor/stabilizer. Then absorbance was monitored continuously for 1 h at 340 nm. PDT and paclitaxel were used as standard destabilizer and stabilizer, respectively for tubulin polymerase [27].

Dichloro-dihydro-fluorescein diacetate (DCFH-DA) and mitochondrial membrane potential (MMP) assay

The procedure is a quantitative method for measuring oxidative stress using flow cytometry, as described by Braicu [28]. In treated and non-treated cells, DCFH-DA dye was added, and after 2 h, fluorescence emission/excitation was observed at 485/530 nm. Similarly, assay measurement was also done through FACS, where cells were seeded in 6-well plates, and treatment was given with neomenthol. DCFH-DA was added, and FACS analyzed the sample within 1 h. MMP is a quantitative method used to determine the permeability of mitochondria by Braicu (2011). The procedure and the analysis of MMP are similar to that of DCFH-DA except for the addition of different dye.

Quantification of PI3K, AKT, mTOR, and HDAC-6 in A431 cells

The PI3K expression was measured by using a commercialized kit procured from Bioassay Technology (Cat. No. E0896Hu). The AKT (Cat. No. 201-12-0893) and HDAC-6 (Cat. No. 201-12-2132) were quantified as per the reported protocol described in the human-specific ELISA kit from Sun Red Company, China. mTOR (Cat. No. E-EL-H1655) was estimated by kit purchased from E Lab Sciences, USA.

In vivo anticancer activity using Ehrlich ascites carcinoma model

The *in vivo* anticancer activity of neomenthol was evaluated in Ehrlich Ascites Carcinoma (EAC) model. The cells were collected from the peritoneal cavity of Swiss albino mice harboring 10–12 days old ascites carcinoma. On day 0, the EAC cells (1×10^7) were injected intra-peritoneal in non-inbred mice selected for the experiment. The next day (day 1), the animals were randomized and divided into five groups including, two treatment groups, one positive control group, one control (only EAC) group, and one healthy group. The first two test groups were treated with 50 and 75 mg/kg, i.p. doses of neomenthol, respectively, from day 1–9. The third group was given 5-fluorouracil at a dose of 20 mg/kg, i.p. from day 1–9, and it served as the positive control, whereas the vehicle (EAC control) group was similarly administered normal saline (0.2 ml i.p.) for 9 days. The fifth group has healthy mice. On day 12, the animals were sacrificed, and ascitic fluid was collected from the peritoneal cavity of each mouse for the evaluation of tumor growth, volume, and weight [29]. The percent tumor growth inhibition was calculated using the following formula.

$$\text{Tumor Growth Inhibition}(\%) = (\text{Average number of tumor cells in the control group} - \text{Average number of tumor cells in the test group}) / \text{Average number of tumor cells in control group} \times 100$$

The microscopic examination of the EAC cells was performed on Day 1, 5, 9, and 12, while the percent survival of the mice was also observed in the groups mentioned above. The percent change in survival (life span) was calculated using the following formula.

$$\text{Change in the Survival (life span)} = ((T - C)/C) * 100$$

where T = number of days the treated animals survived and C = number of days control (EAC) animals survived [30].

The activity of hyaluronidase was also estimated in EAC mice. 200 μL of neomenthol, 5FU treated, and non-treated ascetic fluids were collected in 500 μL of PBS. The samples were mixed and centrifuged at 5000 rpm for 5 min at 4 °C, and the pellet was dissolved in 200 μL RIPA buffer. The protein was estimated as described in the material and methods section. Further, the effect of neomenthol on enzyme activity in EAC cells was observed by following the protocol as described above.

In silico, ex vivo, and acute oral toxicity studies

The chemical and physical properties (ADME) of neomenthol were calculated from Med Chem Software™ version 2.0.0.34 (www.simulations-plus.com), which is mainly for the Lipinski rule of five. Some properties were also retrieved from Pub Chem (https://pubchem.ncbi.nlm.nih.gov/). The *ex vivo* osmotic fragility assay was performed as reported [31]. The test was carried out as per the approved protocol of the Institutional Human Ethics Committee (CIMAP/IHEC/2018/01). The curves were constructed by plotting the lysis percentage against different concentrations

of phosphate-buffered saline, and their hemolytic index was calculated in terms of MEF_{50} (Mean Erythrocyte Fragility). The acute oral toxicity of neomenthol was evaluated following the Organization for Economic Co-operation and Development (OECD) test guideline No 423 (2000) in Swiss albino mice. Neomenthol was suspended in 0.9% NaCl and given through oral route at 300 and 1000 mg/kg of body weight (groups II-IV). Before sacrificing the animals, the blood samples were collected from the orbital venous plexus into the capillary tubes. The serum was separated by the centrifugation at 1000*g* for 5 min and stored at −20 °C until analysis. All the hematological and biochemical parameters (SGOT, SGPT, AKLP, cholesterol, BUN, Bilirubin, Creatinine, HDL, LDL, glucose) were estimated by using an ELISA kit from Siemens, India [27,32].

Ethics statement

All the experiments involving animals were conducted according to the ethical policies and procedures approved by the Institutional Animal Ethics Committees of the CSIR-Central Institute of Medicinal and Aromatic Plants, Lucknow Uttar Pradesh, India (Approval No. CIMAP/IAEC/2019–2021/05, CIMAP/IAEC/2016 (07)-19/32, CIMAP/IAEC/2016–2019/14 and CIMAP/IAEC/2016–2019/01).

Statistical analysis

The *in vivo* data are expressed as Mean ± SE (n = 5). The *in vitro* experiments were performed in replicates (n = 3), and the data are expressed as Mean ± SD. The IC_{50} values were calculated from the dose-responsive curve by using Table curve 2D Windows Version 4.07. The statistical significance of experimental data was calculated by using the one-way analysis of variance, Dunnett test, and student *t*-test ($^{*}p < 0.05$, $^{**}p < 0.01$, and $^{***}p < 0.001$).

Results and discussion

Neomenthol inhibits proliferation of skin cancer (A431) cells

Neomenthol was evaluated for the antiproliferative activity against a panel of organ-specific human cancer and normal cell lines by employing SRB, NRU, and MTT assays. In all the tested assay systems, it was observed that neomenthol exhibited IC_{50} in the range of 16.35 to 99.31 μM. The antiproliferative activity was found better in A431 with an IC_{50} value of 17.3 μM, 18.53 μM, and 82.06 μM in MTT, NRU, and SRB assay respectively compared to other tested cell lines (Table 1 and *Supplementary* Fig. 1). The antiproliferative potential of neomenthol alone has not been reported so far. However, terpene conjugates, including neomenthol, carvomenthol, isolongifolol, and menthol, showed antiproliferative activity against leukemia (HL-60), melanoma (518A2), and colon (HT-29) cancer cells. Also, the propane-1,2-diyl-spaced conjugates of (-)-carvomenthol, (+)-neomenthol, (-)-menthol, and (-)-isolongifolol displayed growth inhibition of melanoma cells at an IC_{50} less than 4 μM [6]. It is reported that menthol retards the growth of melanoma cells via TRPM8 channel activation [33], and a gradual decline in the viable cell population of prostate cancer cells has also been observed with the increase in menthol concentration [34]. Structurally, menthol and its stereoisomer neomenthol possess a similar arrangement of atoms, which confers the difference in their stability; however, neomenthol is amongst the highest stable isomer of menthol. Based on the previous report on menthol antiproliferative potential [35], it was speculated that the pharmacological activity of neomenthol might be similar to menthol. However, the present study confirmed that the antiproliferative potential of neomenthol is better in comparison to reported menthol activity [36]. Also, it was found non-cytotoxic to the human embryonic kidney cell line (HEK-293) at the higher tested concentration (*Supplementary* Fig. 1). Further, among the panel of organ-specific cancer cell lines selected for the study, the cell lines wherein neomenthol exhibit > 30% of the antiproliferative potential in cellular assays (SRB, NRU, and MTT) were opted for studying molecular and cell target based effect of neomenthol.

Neomenthol arrest the G2/M phase and increases sub-diploid cells in skin cancer

Among the tested cancer cell lines, neomenthol arrest different phases of cells in a concentration-dependent manner, followed by an increase in the number of sub-diploid cells. In A431 cells, as the concentration of neomenthol was increased, the number of sub-diploid cells increases and the event proceed towards the apoptotic death of the cells. In MDA-MB-231 cells, neomenthol arrests the S-phase of the cell cycle, which is known for the duplication of the DNA. Comparatively, neomenthol significantly enhanced the apoptosis in the A431 cell line by several-fold (Fig. 1). The arrest of the G0/G1 phase in PC-3 and K562 cell lines was also observed as the stage is responsible for the synthesis of protein, which helps in cell maturation. Earlier reports suggested that menthol caused cell cycle arrest at the G0/G1 phase and inhibited the movement of DU145 (prostate cancer) cells expressing TRPM8 [35]. The G2 and M phases of the cell cycle are responsible for the synthesis of different types of protein and segregation of duplex chromosomes, respectively. The arrest of cells (FaDu, A549, and A431) in the G2/M phase by neomenthol is similar to most of the known inhibitors that arrest the cells in the G2/M phase, following induction of apoptosis [37]. Terpenoids, including farnesol, geranylgeraniol, menthol, and geraniol have been reported to arrest the proliferation of several cell lines and induces apoptosis in several tumor-derived cell lines [38].

Neomenthol inhibits biomarkers of progression, promotion, and initiation phase of the carcinogenesis process

To further establish the potential antiproliferative effect of neomenthol, its efficacy was investigated on different carcinogenesis biomarkers such as COX-2 and LOX-5 (promotion), ODC, Cathepsin D and hyaluronidase (progression), dihydrofolate reductase, and tubulin (initiation). In the antiproliferative assays, the effect of neomenthol was prominent in A431 cells, which support an earlier finding on chemopreventive efficacy of menthol, revealing an unswerving relation to inflammation in skin tumor promotion [36]. The over-expression of COX-2 is responsible for many types of cancer, including breast, colon, lung, and associated with the poor prognosis [39,40], while specifically targeting COX-2 has been reported to reduce the risk of cancer [39,41]. Aberrant expression of LOX-5 has also been reported in various types of human tumors, including the pancreas, prostate, colon, and skin [42]. Thus, the modulation of LOX-5 expression could be an effective strategy for the control of cancer cell proliferation. Therefore, the effect of neomenthol against COX-2 and LOX-5 was studied as a higher expression of these enzymes has been reported in inflammation-related cancer. The results in the present study reveal that neomenthol inhibits the COX-2 activity in the cell lines: A431, MDA-MB-231, PC-3, and FaDu, with the IC_{50} values of 39.09 ± 6.39 μM, 46.16 ± 4.08 μM, 62.25 ± 10.70 μM, and 46.16 ± 4.08 μM respectively.

Moreover, in a cell-free system, neomenthol reduces the enzyme activity with an IC_{50} value of 81.01 ± 0.59 μM (*Supplementary* Fig. 2*A*). Comparatively, the activity of neomenthol against COX-2 was found higher (IC_{50} :39.09 ± 6.39 μM) in A431 cell line

Table 1
IC_{50} value of neomenthol in different cancer cell lines, cell free and cell based assays.

Cell Free Analysis			Cell Based Assay					
Neomenthol		*In vitro*	PC-3	FaDu	A431	K562	MDA-MB-231	A549
	MTT		20.08 ± 0.82	99.31 ± 0.59	17.3 ± 6.49	NA	NA	NA
	NRU		84.61 ± 1.81	NA	18.53 ± 3.66	NA	34.67 ± 9.96	48.07 ± 4.97
	SRB		16.35 ± 3.87	NA	82.06 ± 1.97	NA	NA	NA
	COX-2	81.01 ± 0.59	62.25 ± 10.70	87.19 ± 5.24	39.09 ± 6.39	–	46.16 ± 4.08	–
	LOX-5	–	–	–	–	72.15 ± 2.19	–	–
	ODC	20.2 ± 1.09	–	–	–	29.59 ± 2.54	57.19 ± 2.84	
	CAT D	30.36 ± 6.44	–	74.62 ± 0.21	–	57.47 ± 13.96		62.01 ± 2.08
	HYAL	–	–	–	12.81 ± 0.01	–	–	36.8 ± 5.65
	DHFR	–	–	–	–	–	–	–
Inhibitors / Standards	MTT		02.24 ± 1.56	16.24 ± 1.04	01.60 ± 0.09	46.38 ± 4.27	01.55 ± 0.95	02.10 ± 0.81
	NRU		01.2 ± 0.36	25.34 ± 0.28	01.15 ± 0.37	32.30 ± 3.11	03.64 ± 1.80	01.18 ± 0.13
	SRB		03.0 ± 1.16	34.09 ± 1.79	01.21 ± 0.03	50.26 ± 0.45	01.51 ± 0.86	01.15 ± 0.16
	Celecoxib	02.39 ± 0.21	04.28 ± 0.36	30.70 ± 7.07	11.65 ± 4.68	35.61 ± 6.21	17.49 ± 7.06	38 ± 7.04
	Zileuton	01.1 ± 0.04	01.73 ± 0.04	26.15 ± 0.28	07.88 ± 0.70	07.09 ± 0.98	01.77 ± 0.06	37.75 ± 5.48
	DFMO	07.54 ± 5.8	15.54 ± 0.56	09.80 ± 1.87	11.15 ± 4.50	07.67 ± 1.63	08.02 ± 1.82	10.53 ± 2.63
	PEP A	06.75 ± 0.53	08.34 ± 2.10	09.11 ± 3.79	09.34 ± 0.05	08.99 ± 1.28	03.84 ± 0.76	14.10 ± 1.40
	NAC	05.92 ± 0.70	09.44 ± 3.13	07.44 ± 0.67	08.20 ± 1.42	07.56 ± 0.59	14.61 ± 3.07	13.73 ± 4.37
	MTX	12.65 ± 2.06	10.24 ± 2.90	07.19 ± 3.65	30.96 ± 6.90	21.1 ± 12.3	08.19 ± 3.04	08.19 ± 4.17

NA- Not active. Cell specific standards were used i.e. Doxorubicin for MDA-MB-231, PC-3, A431, Taxol for A549 and Podophyllotoxin for FaDu, K562. COX-2: Cyclooxygenase, LOX-5: Lipoxygenase, ODC: Ornithine decarboxylase, CAT D: Cathepsin D, HYAL: Hyaluronidase, DHFR: Dihydro folate reductase, DFMO: α-difluoromethylornithine, PEP A: pepstatin A, NAC: N-acetyl cysteine, MTX: Methotrexate.

(Table 1). Further, the molecular docking interaction analysis confirms the binding of neomenthol with the COX-2 receptor; however, the binding pocket and the interacting amino acid residues present in the 4 Å proximity is different to that of celecoxib (Table 2, *Supplementary* Fig. 3*A, 3B*), which suggest another binding pocket for neomenthol. These results were further confirmed with the real-time expression analysis. Neomenthol down-regulated the expression of prostaglandin-endoperoxide synthase, COX-2 activity in most of the tested cell lines, except K562.

In contrast, higher affinity was observed for A431 and FaDu cells with 1.34 and 1.38 fold change, respectively (Table 3 and *Supplementary* Fig. 4). Our results are in agreement with the findings of Juergens [43], who showed that L-menthol significantly suppresses the over-expression of inflammation biomarkers such as leukotriene (LTB-4), prostaglandin E2 (PGE-2), and interleukin-IL-1-b (pro-inflammatory cytokines) involved in the immune defense against infection caused by the monocytes. These inflammatory mediators concentrations indicate activation of cyclooxygenase and lipoxygenase signaling pathways in cells [44].

Neomenthol reduced the LOX-5 activity in both cell-free and cell-based system (s) in the tested cell lines. However, a significant decrease was observed only in the K-562 cell line with an IC_{50} value of 72.15 ± 2.19 μM (Table 1, *Supplementary* Fig. 2*B*). From the drug-receptor interaction analysis, it was confirmed that neomenthol binds with LOX-5; however, the binding site was different from that of zileuton (Table 2, *Supplementary* Fig. 3*C and D*). The real-time expression analysis further validated the *in vitro,* and molecular docking results wherein neomenthol did not down-regulate the expression of LOX-5 significantly in most of the tested cell lines. The fold change of LOX-5 was observed only in three cell lines (A431, FaDu, and K562); interestingly, the fold change of LOX-5 was approximately similar in A431 (1.25) and FaDu (1.26) as shown in Table 3 and *Supplementary* Fig. 4. Thus, our results reveal that neomenthol modulates the LOX-5 activity as well as down-regulate LOX-5 mRNA expression in cells, and similar to menthol, neomenthol showed a potential effect against COX-2 than LOX-5 [36].

During carcinogenesis, an elevated level of polyamine concentration has been reported, which causes an accelerated cellular transformation. Ornithine decarboxylase (ODC) is primarily involved in the biosynthesis of polyamines and is reported to be associated with the modulation of the inflammatory enzyme such as COX-2 and LOX-5. Thus, inhibiting the regulatory enzyme (ODC) of the polyamine biosynthesis has been observed as a remarkable step to inhibit cell proliferation and transformation [20]. The over-expression of cathepsin D (CATD) in cancer plays a vital role in tumor invasion at distant sites. The secretion of CATD is indirectly regulated by tetrahydrofolate, a product formed by the action of dihydrofolate reductase (DHFR). Hence, CATD is one of the persuasive biomarkers for the discovery of novel and specific anticancer agents [45]. At the site of inflammation, hyaluronidase gets accelerated and degrade the higher level of hyaluronan (HA) present in the skin, to modulate the invasion of tumor cells and angiogenesis [46]. Therefore, it could be a prominent marker for neomenthol to deregulate/inhibit the process of carcinogenesis.

Neomenthol inhibited the activity of ODC in both cell-free and cell-based test systems with the decreasing order: cell-free > K562 > MDA-MB-231 > A549 > A431 > PC-3 > FaDu. Neomenthol retard the enzyme activity by ~ 50% in the cell-free system with IC_{50} 20.2 ± 1.02 μM while in K562 and MDA-MB-231 cell lines it showed the IC_{50} value 29.59 ± 2.54 μM and 57.2 ± 2.85 μM, respectively. The percent inhibition was below 50% in A549, PC-3, A431, and FaDu, cell lines (Table 1; *Supplementary* Fig. 2*C*). The inhibitors of ODC are reported to be heat-labile, and its induction is primarily dependent upon the protein synthesis [47]. The inhibitors of ODC are effective against various murine skin models. However, when translated to humans, the effect of ODC inhibitors was not as substantial as depicted by the pre-clinical studies [48]. Neomenthol imparts a cooling effect on the skin; therefore, its modulatory effect may be due to targeting ODC, which then retards the growth of skin cells. The molecular docking studies indicated a strong interaction of neomenthol with ODC as compared to DFMO (*Supplementary* Fig. 3*E and F*), but the binding pockets were not similar (Table 2). The real-time qPCR expression analysis showed that neomenthol down-regulate the expression of ODC in all the tested cell lines except K562, which does not coincide with the *in vitro* results; the highest fold change (1.22) was observed in PC-3 cell lines (Table 3 and *Supplementary* Fig. 4). Our experimental findings are in agreement with the findings of Carnesecchi (2001), reporting that terpenoids decrease the ODC activity in cancer cells [49].

The concentration-dependent effect of neomenthol against CATD in different cell lines has been depicted in *Supplementary* Fig. 2*D,* and the order of inhibition of the enzyme activity was observed as FaDu > A549 > K562 > PC-3 > MDA-MB-231 > A431.

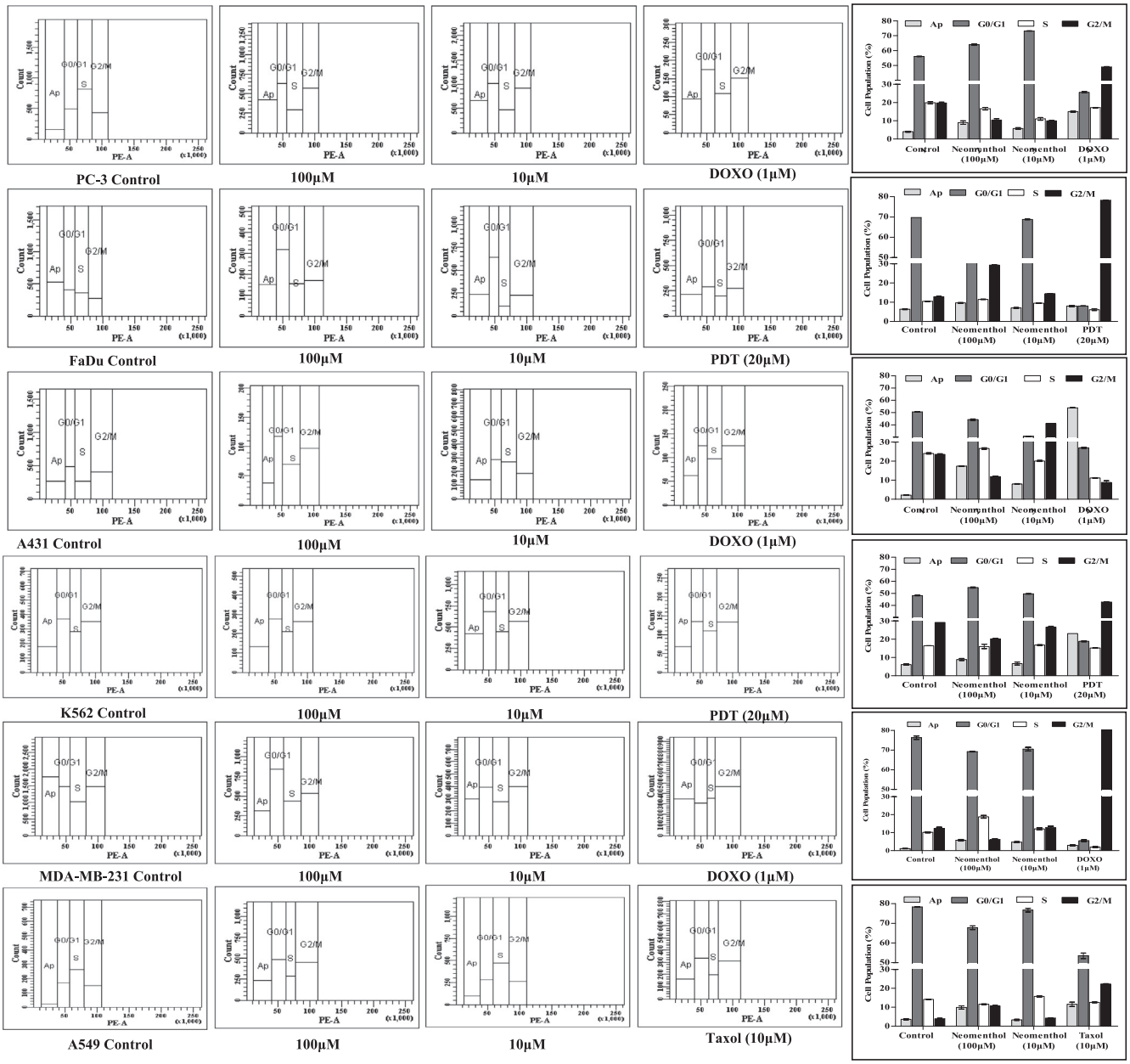

Fig. 1. Cell cycle analysis results of neomenthol in different cancer cell lines by using flow cytometry. PC-3, A431, FaDu, K562, MDA-MB-231, and A549 were treated with indicated concentrations of neomenthol for 24 h and stained with PI to determine DNA fluorescence and cell cycle distribution as described in material and methods section. Data were analyzed by FACS Diva software for the proportions of different cell cycle phases. The fraction of cells from apoptosis, G1, S and G2 phases analyzed from PE-A vs cell counts are shown in (%). Data expressed as mean ± SD. The arrest and apoptosis of each cell line was also represented in column. Cell specific standards were used i.e. doxorubicin (DOXO) was used for MDA-MB-231, PC-3, A431, taxol was used for A549 and podophyllotoxin (PDT) was used for FaDu and K562.

In FaDu, A549, and K562 cell lines, neomenthol decreased the activity of the enzyme with the IC_{50} value 79.62 ± 0.21 µM, 62.01 ± 2.08 µM, and 57.47 ± 13.96 µM respectively, whereas in other tested cell lines: PC-3, MDA-MB-231, and A431, it moderately affects the enzyme activity (Table 1). The binding affinity of neomenthol with CATD was observed lower compared to pepstatin A. However, the amino acid residues (GLY 79.A, MET 309.B, ASP 231.B) are common in 4 Å vicinity of the protein to which neomenthol and pepstatin A binds, which suggests similar binding pockets (Table 2, *Supplementary* Fig. 3*G, H*). The real-time qPCR expression analysis revealed that neomenthol down-regulates the expression of CATD in the tested cell lines (Table 3), and the highest fold change of CATD by neomenthol was observed in both PC-3 and A549 as depicted in *Supplementary* Fig. 4. Our experimental findings are in agreement with the work of Majumdar (2011), reporting that natural products decrease the cathepsin activity in cancer cells [50].

The order of inhibition of hyaluronidase activity by neomenthol was A431 > A549 > MDA-MB-231 > K562 > PC-3 > FaDu cell lines (*Supplementary* Fig. 2*E*). The modulation of hyaluronidase activity by neomenthol was higher in A431 and A549 cells with the IC_{50} values 12.81 ± 0.01 µM and 36.8 ± 5.65 µM, respectively (Table 1). However, in the cell-free system, neomenthol inhibits the enzyme activity by 24.9 ± 4.31%. The molecular docking interaction study depicts a strong binding of neomenthol within the active site of the hyaluronidase, and the binding of neomenthol was stronger than NAC (*Supplementary* Fig. 3*I and J*). The interaction of neomenthol with the amino acid residues was different to NAC (Table 2).

Further, the *in vitro*, cell-free, and cell-based results were verified using the real-time expression studies. The results revealed

Table 2
Binding energy (B.E), inhibition constant (Ki), interacting amino acids and residues forming hydrogen bond in 4 Å radius for neomenthol against selected targets/biomarkers for cancer.

Targets	PUB ID/ PubChem CID	B.E (Kcal/mol)	Ki	Residues within region of 4 Å radius	H - bonds forming residues bond length in Å
COX-2	5IKQ	−5.87	49.97 μM	TYR373.A, GLN 375.B, GLY 536.A, GLN 374.A, ASN 375.A, HIS 226.A, GLY 225. A, GLY 227.A, VAL 538.A, ASN 537.A, PHE 143.B, TRP 140.B, HIS 226.A, GLY 225.A,VAL 228.A, PRO 128.B, ASN 375.B	2.78 Å with GLY225.A
Celecoxib	2662	−7.59	2.71 μM	LYS 533.B, GLN 375.B, ARG 377.B, ASN 376.B, LEU 146.B, HIS 227.B, GLY 226.B, GLY 228.B, ASP 230.B, GLY 537.B, LYS 533.B, PRO 129.B, GLY 534.B, ASN 376.B, PHE 142.A, VAL 539.B, TRP 139.A, ASN 538.B, GLY 375.B, SER 143.A, ASP 230.B	2.69 Å, 2.59 Å with ARG 377.B; 2.98 Å with TRP139.A
LOX-5	3O8Y	−5.69	67.70 μM	ASP 290.B, LYS 441.A, GLN 329.B, ARG 520.A, LYS 254.B, MET 440.A, ARG 520. A, ILE 330.B, ARG 518.A, GLY 150.A	2.75 Å, 3.20 Å with ARG 518.A; 2.73 Å with ASP 290.B
Zileuton	60490	−6.27	25.28 μM	PRO 149.B, GLN 434.B, GLN 437.B, ARG 438.B, LYS 441.B, ARG 438.A, GLY 291. A, ASP 290.A, GLN 434.A, GLN 437.A, LYS 441.B, LYS 441.B, GLY 150.B	2.57 Å with GLN434.B; 2.68 Å, 2.63 Å with GLN 437.A
ODC	4ZGY	−5.57	82.82 μM	SER 191.B, PHE 192.B, TYR 331.A, ARG 188.B, TYR 389.A, ASP 332.A, ARG 277. A, SER 200.A	2.79 Å with ARG 277.A ; 3.03 Å with ASP 332.A
DFMO	3009	−4.11	969.97 μM	GLU 196.B, PHE 397.A, SER 395.A, THR 396. A, ALA 392.A, ASP 72.A	2.60 Å, 2.67 Å with GLU 196.B; 2.87 Å, 2.93 Å, 3.05 Å with THR 396.A
CAT D	4OBZ	−4.88	265.04 μM	TYR 278.A, GLY 81.A, **GLY 79.A**, TYR 78.A, SER 80.A, **MET 309.B**, ILE 320.B, **ASP 231.B**, GLY 233.B, VAL 238.B, THR 234.B, SER 235.B, THR 125.B	Not formed probably due to the residues are not present in close proximity
PEP A	5478883	−16.97	1 pM	SER 315.B, TYR 205.B, ILE 142.B, TYR 78.A, GLY 79.A, HIS 77.A, PRO 173.D, ASP 231.B, TYR 312.B, ILE 311.B, MET 309.D, GLY 75.A, GLY 36.A, LYS 8.B	2.64 Å with TYR 205.B; 2.93 Å with SER 315.B; 2.69 Å and 2.66 Å with LYS 8.B
HYAL	2PE4	−5.82	54.90 μM	GLU 131.A, TYR 247.A, TRP 321.A, ILE 73.A, ASN 37.A, TYR 286.A, TYR 75.A, VAL 127.A, TYR 75.A, ASN 37.A, ASP 129.A, TYR 202.A	2.66 Å with ASP 129.A
NAC	12035	−4.38	611.11 μM	ARG 244.A, VAL 226.A, SER 225.A, ALA 185.A, TYR 184.A, TYR 227.A, GLN 271.A	3.23 Å with GLN 271.A; 3.02 Å with TYR 227.A; 2.70 Å with SER225.A
DHFR	4QHV	−4.45	546.42 μM	ARG 36.A, THR 40.A, MET 37.A, ASN 48.A, TRP 113.A, PHE 134.A, MET 111.A, TYR 162.A	2.78 Å with MET 37.A; 2.85 Å with THR 40.A
MTX	126941	−9.80	65.77 nm	PRO 26.A, LEU 27.A, ARG 32.A, PRO 25.A, PHE 31.A, GLN 35.A, LEU 22.A, LEU 67.A, PHE 34.A, ARG 70.A, THR 38.A, VAL 115.A, VAL 50.A, TRP 24.A, ILE 60.A, ILE 51.A, ILE 114.A, MET 52.A, GLU 30.A	2.34 Å with GLU 30.A
Tubulin	1TUB	−7.20	5.26 μM	**PRO 173.A, ALA 174.A, GLN 176.A, TYR 172.A, GLU 207.A**, TYR 210.A, LYS 326. B, MET 325.B, VAL 77.A, **ASN 206.A, SER 178.A, TYR 224.A, ASP 329.B**	Å with TYR 224.A;3.21Å with ASP 329.B
PDT	10607	−10.44	22.17 nm	ALA 12.A, LEU 248.B, ILE 171.A, GLY 142.A, TYR 224.A, PRO 173.A, PHE 141.A, VAL 182.A, GLN 176.A, TYR 172.A, VAL 177.A, ASN 206.A, ASP 329.B, GLU 207. A, ALA 174.A, SER 178.A	2.72 Å with SER 178.A

COX-2: Cyclooxygenase, LOX-5: Lipoxygenase, ODC: Ornithine decarboxylase, CAT D: Cathepsin D, HYAL: Hyaluronidase, DHFR: Dihydro folate reductase, DFMO: α-difluoro methyl ornithine, PEP A: pepstatin A, NAC: N-acetyl cysteine, MTX: Methotrexate, PDT: Podophyllotoxin. # BOLD indicates the amino acids alike with standards.

Table 3
mRNA expression level among different cancer cell lines and selected targets/biomarkers.

	Control	COX-2	Celecoxib	LOX-5	Zileuton	HYAL	NAC	ODC	DFMO	CAT D	PEP A	DHFR	MTX
PC-3	1	1.19	2.19	NA	2.22	1.37	5.64	1.22	6.55	1.35	1.66	NA	2.0
FaDu	1	1.38	2.45	1.26	2.96	1.06	6.66	1.08	2.57	1.31	2.22	NA	2.82
A431	1	1.34	3.29	1.25	3.10	1.52	4.50	1.15	5.42	1.19	1.61	NA	2.92
K562	1	NA	2.69	1.10	3.01	NA	8.98	NA	4.07	1.24	3.12	NA	2.20
MDA-MB-231	1	1.16	2.86	NA	3.09	NA	6.87	1.05	3.67	1.15	1.81	NA	2.59
A549	1	1.09	1.90	NA	1.77	NA	4.09	1.18	4.24	1.37	2.77	1.17	2.20

COX-2: Cyclooxygenase, LOX-5: Lipoxygenase, ODC: Ornithine decarboxylase, CAT D: Cathepsin D, HYAL: Hyaluronidase, DHFR:Dihydrofolate reductase, DFMO: α-difluoromethylornithine, PEP A: pepstatin A, NAC: N-acetyl cysteine, MTX: Methotrexate, GAPDH was Internal Control. The expression level is indicated by fold change of neomenthol with respect to control. NA: Not Active.

that neomenthol increases the level of hyaluronidase by 1.52 and 1.37 fold in A431 and PC-3 cell lines, respectively (Table 3 and *Supplementary* Fig. 4). These results validated the *in vitro* and *in silico* outcome. It is known that about 50% of HA ispresent in the skin which is degraded by hyaluronidase. It further results in enhancing skin permeability, adhesion, and angiogenesis. Since menthol affects the skin cells [3,4], neomenthol being an isomer of menthol could also retard the growth of the skin cancer cell line by targeting the hyaluronidase activity. It is likely possible that neomenthol affects the proliferation of skin cancer cells via two plausible mechanisms; (i) neomenthol is a moderate hydrophobic and lipophilic molecule, and according to Lipinski rule of five, these types of molecule easily cross the plasma membrane. Probably, while crossing the plasma membrane, it may interfere with the lipid structure where HA is localised or disturb the hyaluronidase structure due to which hyaluronidase unable to cleave β-D1,4 linkage; hence resists HA fragmentation (ii) neomenthol might be distressing the mitochondrial enzyme of A431 cells depicted in MTT and MMP assays, it indirectly inhibited COX-2 activity, which in turn impede hyaluronidase activity and ultimately prevents the degradation of HA [51]. Conclusively, neomenthol inhibits the activity of COX-2 (IC_{50} 39.09 ± 6.39 μM) and hyaluronidase (IC_{50} 12.81 ± 0. 01 μM) in A431 cells with a prominence more towards hyaluronidase, wherein HA is not degraded and which might results in a decrease in permeability, adhesion, and angiogenesis of the cells, and eventually, the skin cells undergo apoptosis.

Dihydrofolate reductase (DHFR) plays a vital role in cell proliferation by maintaining the tetrahydrofolate level. Furthermore, inhibiting DHFR activity limits cell growth and proliferation, which is amongst the characteristics of cancer cell [52]. DHFR reduces dihydro folic acid to tetra hydro folic acid, using NADPH as an electron donor. Tetrahydrofolate is used in a variety of biochemical reactions involving single carbon transfers at various oxidation states. It is a methyl group shuttle essential for *de novo* biosynthesis of DNA bases. Also, its deficiency has been linked with megaloblastic anemia, and hypersecretion causes malignancy. In results, neomenthol did not show any significant activity in both cell-free or cell-based systems (Table 1, *Supplementary* Fig. 2*F*). However, neomenthol showed interaction with DHFR in *in silico* experiment, but the affinity was not as strong as methotrexate (MTX), and the binding pockets were not similar. MTX is a large molecule having three cyclic rings; thus, it can easily fit in the active site of the enzyme, and the residues (histidine and arginine) help in the strong binding of MTX with DHFR [53]. In contrast, neomenthol is a small molecule with only a single ring which makes it unable to fit in the active site of the enzyme (low affinity towards DHFR) as observed in the molecular docking interaction studies (Table 2, *Supplementary* Fig. 3*K, L*). In the real-time qPCR analysis, fold change of DHFR by neomenthol was almost negligible in the tested cell lines except for A549, wherein the fold change was non-significant (1.17, Table 3 and *Supplementary* Fig. 4).

Since microtubule function is most prominent in mitosis (M phase) and cell cycle results showed neomenthol arrest G2/M phase in A431 cells. Hence to reconfirm the cell cycle analysis data, neomenthol efficacy was further tested on the microtubule functions by performing tubulin polymerization assay. The microtubule array dynamics is responsible for establishing a bipolar mitotic spindle which acts to segregate the replicated chromosomes into daughter cells during cell division. The regulation of the dynamic instability is critical during mitosis for the bipolar attachment of the microtubules to each chromosome, alignment of the chromosomes at the metaphase, signaling at the anaphase transition, and chromosome separation at the telophase. Disruption in these processes leads to mitotic arrest and cell death [37]. The experimental data is depicted as the kinetic graph in Fig. 2, wherein podophyllotoxin (PDT, 10 μM) and neomenthol (100 μM) was observed to inhibit the polymerization of α and β tubulin, an effect which was concentration-dependent, whereas paclitaxel (10 μM) stabilizes the tubulin polymerization. Thus, it is hypothesized that neomenthol arrests the G2/M phase of skin cells by averting the polymerization of tubulin dimmers, which might disturb the dynamic property of the cells leading to apoptosis. The molecular docking studies further confirm the interaction of neomenthol with tubulin, however not better in comparison to PDT (*Supplementary* Fig. 3*M* and *N*). Also, the binding pockets were similar

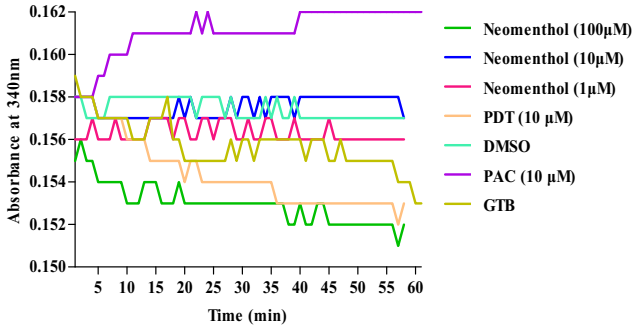

Fig. 2. Neomenthol inhibits tubulin polymerization. Neomenthol was incubated with general tubulin buffer (GTB) at indicated concentration and the kinetic study was performed by using UV–Vis spectrophotometer. Paclitaxel (PAC) was used as tubulin stabilizer and podophyllotoxin (PDT) was used as tubulin destablizer.

for both neomenthol and PDT (Table 2). This observation is in agreement with the earlier finding, which depicts that L-menthol causes apoptosis in human colon adenocarcinoma with enhanced tubulin polymerization [54]. Besides, tubulin also plays a role in transporting intracellular HA to the nucleus wherein HA binds to spindle fiber and helps in the segregation of the chromosome [51]. The molecular docking interaction studies and tubulin polymerization assay showed that neomenthol act as a tubulin polymerization inhibitor due to which tubulin may not be able to transport HA to the nucleus; hence the daughter cells could not be formed.

Neomenthol induces apoptosis by disrupting the mitochondrial membrane potential (MMP) and increasing ROS

Since neomenthol-induced antiproliferative potential was better in A431 cells, the effect of neomenthol on intracellular ROS production and changes in MMP potential was determined in A431 cells. The ROS production is a mechanism shared by all non-surgical therapeutic approaches for cancers, including chemo, radio, and photodynamic therapy, due to itsinvolvement in triggering cell death [55]. The level of ROS was increased in a concentration-dependent manner, and the percent increase in the ROS level was 20.45 ± 0.35% at the highest concentration. Similarly, in the case of flow cytometric analysis, the cell populations shifted from red to green channel, indicating an increase in the number of DCF positive cells (Fig. 3). The total mean of DCF positive cells was 255.5 ± 0.71 μM, 249 ± 7.07 μM at 100 μM and 10 μM, respectively compared to the untreated control (201 ± 1.41). Doxorubicin was used as a positive control and found to increase DCF positive cells (370 ± 14.14) at 1 μM. The increase in the ROS level by neomenthol supports the finding of monoterpenes inducing oxidative stress by the intracellular accumulation of reactive oxygen species [56].

The disruption of mitochondrial membrane potential ($\Delta\Psi m$) is amongst the earliest intracellular events that occur following the onset of apoptosis [29]. Neomenthol decreased the potential of mitochondrial membrane, and the percent decrease concerning control was 13.05 ± 2.6%, at the highest concentration. Similar results were also observed in flow cytometric analysis. The cell populations shifted from red to green channels, indicating a concentration-dependent decrease in the potential of the mitochondrial membrane (Fig. 4). The total of FITC mean was 2913 ± 1.41, 3101 ± 1.41 at 100 μM and 10 μM respectively compared to the untreated control (3194.5 ± 2.12). Doxorubicin was used as a positive control and found to disrupt the mitochondrial membrane potential (2735 ± 5.65) at 1 μM. The loss of mitochondrial membrane potential is a premature apoptotic event that disturbs the downward signals which instigate the intrinsic apoptotic death. Neomenthol decreases the skin cell proliferation shown by MTT assay, which is based on the principle of reduction of mitochondrial succinate dehydrogenase, correlates with the result of MMP wherein neomenthol damages the mitochondrial membrane.

Neomenthol does not induce apoptosis by PI3K/AKT/mTOR pathway and HDAC-6 activity

The PI3K/AKT/mTOR signaling pathway is a key regulator of cellular processes involved in cell growth, proliferation, metabolism, motility, survival, and apoptosis. These pathways are activated either by the receptor tyrosine kinase or the cytokine receptor or G-protein coupled receptor, which activate transcription factor and, in turn, activate HA, which is responsible for the growth of normal cells. However, aberrant activation of the PI3K/AKT/mTOR pathway promotes the survival and proliferation of tumor cells [29,57]. The HDAC-6 deacetylate the acetyl group of the lysine present in

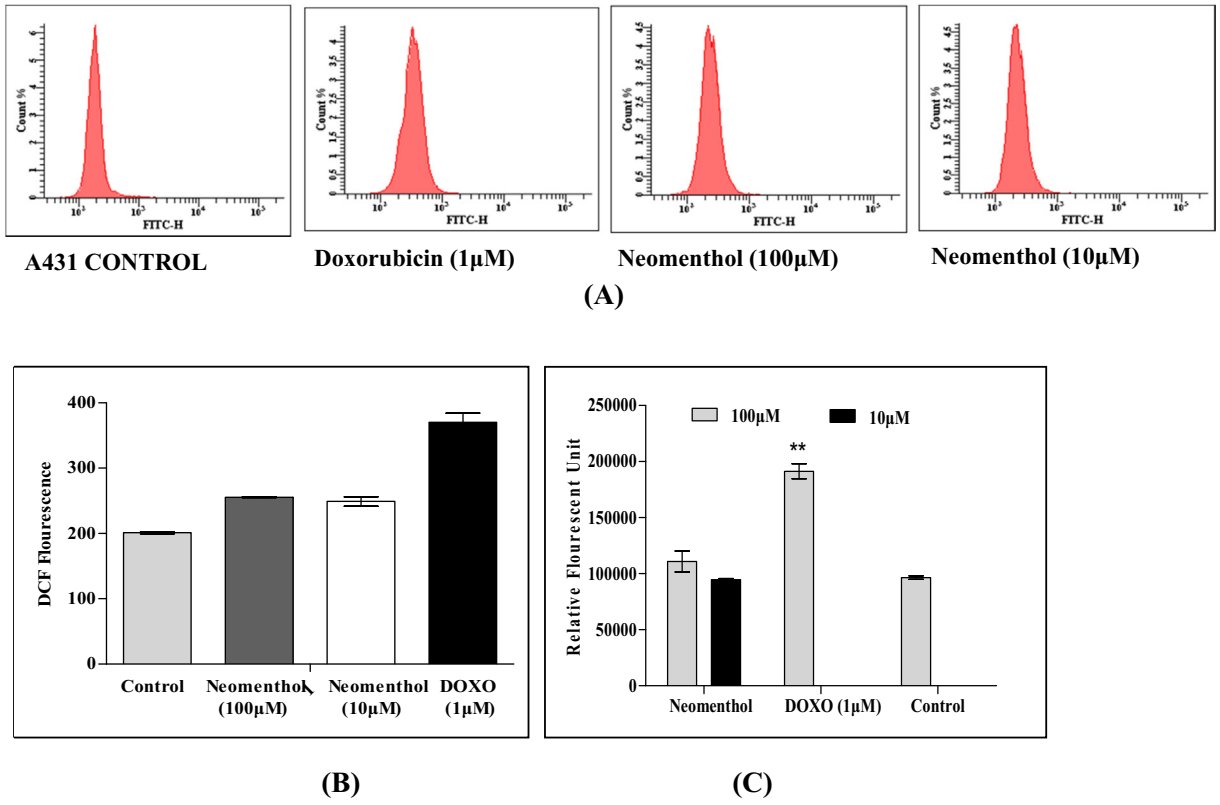

Fig. 3. Neomenthol increases ROS level in A431 cell line. (A) The DCFH-DA staining was used to detect ROS production in A431 cell line at indicated concentrations and analyzed by flow cytometry (B) flow cytometry results (C) A431 cells were treated with neomenthol at indicated concentration in 96-well plate for 24 h then incubated with 10 µM DCF-DA, analyzed by spectrofluorometer. Doxorubicin was used as the positive control. The data are presented as mean ± SD. Neomenthol was compared with control using one way ANOVA via Dunnett test through Graphpad Instat Software. (Non-significant changes were observed).

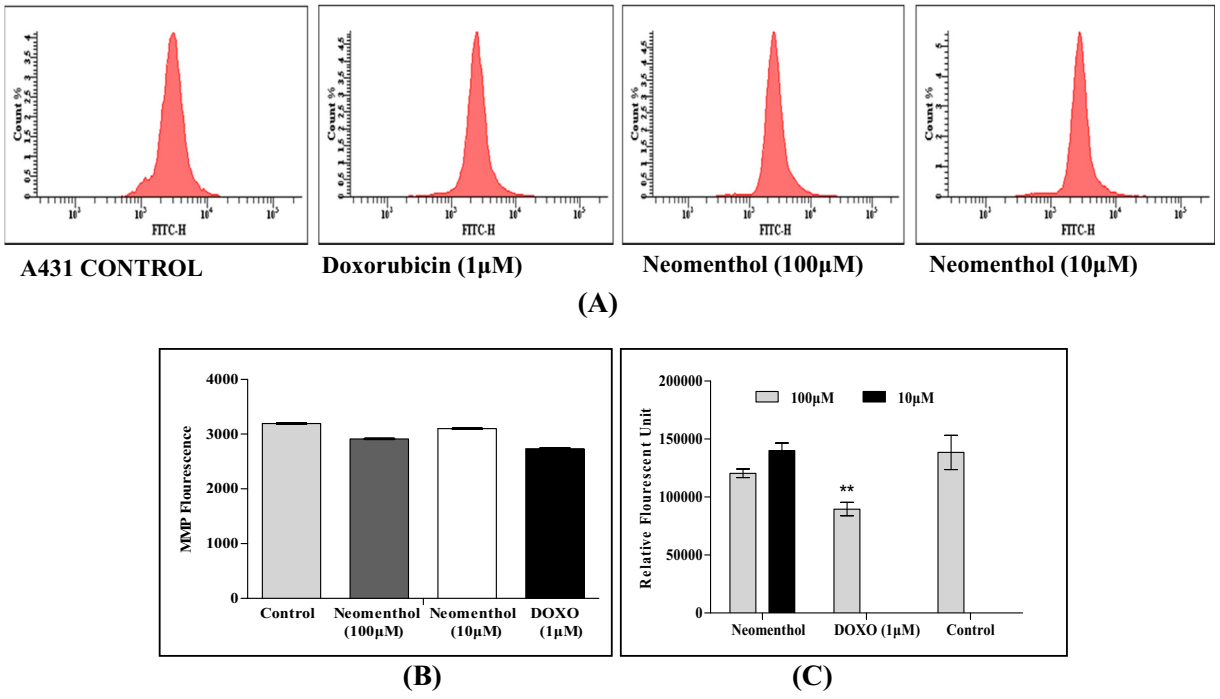

Fig. 4. Neomenthol decreases the mitochondrial membrane potential of A431 cell line. (A) Neomenthol pre-treated A431 cells were incubated with 10 µM Rh123, within 1 h analyzed by flow cytometry (B) flow cytometry results (C) A431 cells were treated with neomenthol at indicated concentration in 96-well plate for 24 h then incubated with 10 µM Rh123, analyzed by spectrofluorometer. Doxorubicin was used as the positive control. The data presented are mean ± SD. Neomenthol was compared with control using one way ANOVA via Dunnett test through Graphpad Instat Software (Non-significant changes were observed).

the histone protein, which enhances histone proteins positive charge. It then attracts negative charge phosphate backbone of DNA. This process allows tight winding of DNA with histone to facilitate chromatin fitting, which is necessary for cell duplication. The HDAC-6 contributes to cancer metastasis as its up-regulation increases cell motility [58]. Therefore, the ability of neomenthol against the key regulator enzyme was investigated, and it was found that neomenthol inhibits the activity in a concentration-dependent method. The data was expressed in terms of ng/mg of protein and at higher concentration (100 μM), neomenthol reduced the activity of PI3K (0.006 ± 0.00021 ng/mg), AKT (0.125 ± 0.004 ng/mg), mTOR (0.336 ± 0.108 ng/mg), and HDAC-6 (0.104 ± 0.001 ng/mg). Surprisingly, the inhibition of these pathways was not significant compare to control (Fig. 5). This finding suggests that neomenthol may not degrade HA by targeting these pathways. Our observation coincides with the earlier report depicting that phytochemicals induce apoptosis by the inactivation of AKT in human colon cancer cells [59], and natural products might play an important role in inhibiting the signaling of PI3K/AKT/mTOR in cancer cells.

Neomenthol retards the growth of the tumor in the Ehrlich ascites carcinoma (EAC) model

To further confirm the *in vitro* antiproliferative potential of neomenthol, its efficacy was evaluated *in vivo* using the EAC mice model. The EAC is a well-established model in tumor biology, which is extensively used to study the tumor pathogenesis and the discovery of anticancer agents [60]. The murine model of ascites EAC provides a reliable means of qualifying *in vivo* antitumor severity that correlates with *in vitro* cytotoxicity. Neomenthol showed significant *in vivo* prevention of tumors compared to the untreated control (i.e., EAC). It reduces 58.84% EAC tumor cells at 75 mg/kg and 23.98% at 50 mg/kg bw *i.p.* dose. However, the standard drug 5-fluorouracil exhibited potential activity at 20 mg/kg bw by reducing 98.39% tumor formation (Fig. 6**A and B**).

Meanwhile, we also observed the effect of neomenthol on the survival (life span), and the bodyweight of EAC harbored mice. We observed that EAC harbored mice (untreated group) died within 24 days (50% mice died on 21 days, and another 50% mice died on 24 days) whereas neomenthol (75 mg/kg body weight) treated group animal survived till 27 days (25% mice died on 24 days, 50% mice died on 26 days and 25% mice died on 27 days). Thus, the survival rate of neomenthol treated mice was 17% higher compared to EAC harbored mice. After 05 days, a continuous increase in the bodyweight of EAC harbored mice was noticed till the animal survives (21 days); however, a decline in the bodyweight of neomenthol treated mice was perceived after 12 days, indicating the reduction in tumor cell growth. A non-significant change was observed in the bodyweight of 5FU treated mice from day 1 to day 24 (Fig. 6**C** and Fig. 6**D**). The microscopic examination of EAC harbored peritoneal fluid revealed consistent increase in the number of tumor cells on day 1 < 5 < 9 < 12 while in the neomenthol treated group, there was a decrease in the number of tumor cells on days 5, 9, and 12 with a significant number of dead cells was observed on 9th and 12th days (Fig. 6**B and E**). There was no mortality of animals in a healthy group until the completion of the experiment. To the best of our knowledge and understanding, no report has been published showing inhibition or prevention of EAC tumors by neomenthol. Still, information on tumor incidence was found to be lower in DMBA/TPA-induced skin tumorigenesis model in female ICR mice by menthol. The effect of neomenthol on hyaluronidase activity in EAC cells was also observed. It was found that neomenthol modulates the enzyme activity up to 10% in EAC cells of mice. A higher expression of hyaluronidase in breast, prostate, bladder, pancreas cancer cells has been reported; however, no report is available on the modulation of hyaluronidase activity in EAC cells, which may either be due to lesser hyaluronidase expression or feeble interaction of hyaluronidase with natural products [61–63]. Therefore, neomenthol did not significantly inhibit the hyaluronidase activity in EAC cells of mice.

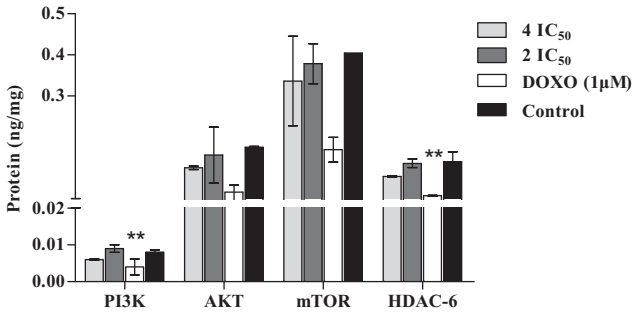

Fig. 5. Neomenthol modulates cell proliferation pathways in A431 cell line. A431 cells were incubated with the indicated dose of neomenthol for 24 h then crude protein from these cells was collected using lysis buffer. Estimation was done as per the instructions given in ELISA kit manual (PI3K, AKT, mTOR, HDAC-6, X axis). Doxorubicin (DOXO) was used as the positive control. The data was estimated as ng/mg of protein (Y Axis). All values are in mean ± SD. Treated samples were compared with control using one way ANOVA via Dunnett test through Graphpad Instat Software. (Non-significant changes were observed).

Neomenthol shows acceptable drug-likeness property and safe up to 1000 mg/kg body weight in mice

Neomenthol was evaluated for its physico-chemical properties such as absorption, distribution, metabolism and excretion (ADME). The log P value indicates hydrophobicity and lipophilicity [64]. The analysis revealed that neomenthol follows Lipinski's rule of five which indicats its good bioavailability potential. Its molecular weight is lower than 500, hydrogen bond donor (1), acceptor (1), and logP values is less than 5 (*Supplementary* Table 2). It suggests that neomenthol possesses good hydrophobicity with moderate lipophilicity and therefore, can cross the plasma membrane. Due to its moderate lipophilicity, it may easily reach the receptor site. The solubility (Log S) of a molecule significantly affects its absorption and distribution characteristics, and the Log S value of neomenthol was within the acceptable range, suggesting it as a safe molecule.

The effect of neomenthol was further confirmed by performing the osmotic fragility test in human erythrocytes. A non-significant change was observed in the osmotic lysis test when erythrocytes were placed in an isotonic and hypotonic solution of increasing strength [31]. Neomenthol was found non-toxic to erythrocytes (*Supplementary* Fig. 5) and its percent mean erythrocyte fragility (MEF_{50}) was similar to control. Therefore, neomenthol is considered safe for erythrocytes at 100 μM.

In the acute oral toxicity experiment, there were non-significant changes, morbidity, and mortality recorded throughout the experimental period at 300 and 1000 mg/kg body weight of mice. A non-significant difference was observed in body weight, hematological, and serum biochemical parameters. The mice under study showed no change in organ weight (*Supplementary* Fig. 6). The blood and serum analysis revealed a non-significant difference in all the tested parameters, including total hemoglobin level, RBC count, WBC count (*Supplementary* Fig. 7), liver function test (SGPT, SGOT, ALP), kidney function test (creatinine, BUN, albumin), lipid profile (triglycerides, cholesterol, HDL, LDH), total and direct bilirubin (*Supplementary* Table 3) compare to control mice group. The data conclude that neomenthol is non-toxic upto 1000 mg/kg body weight in the Swiss albino mice. However, Oz et al., (2017) reported a very low acute oral toxicity of menthol isomers with

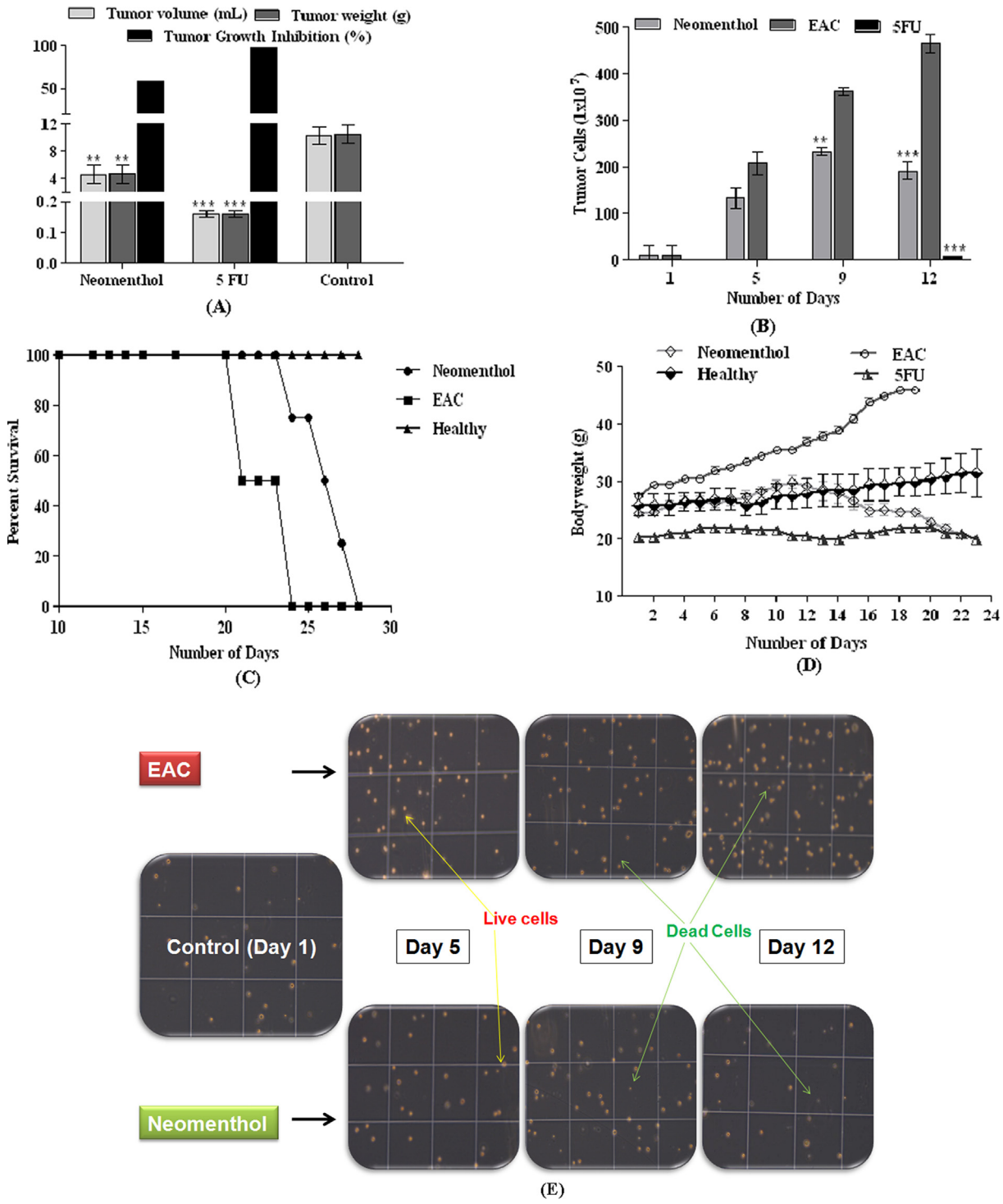

Fig. 6. EAC tumor reduction by neo-menthol in Swiss albino mice. One day after tumor induction in mice (i.p.), neomenthol was administrated intra-peritoneal to the animals for 9 days and tumor was evaluated on day 13. NaCl (0.9%) was given as vehicle to the control group and 5FU (5 fluorouracil) was used as the positive control. (A) Tumor volume, weight and inhibition (B) Tumor cells (C) Percent survival (D) Body weight and (E) Microscopic images of EAC cells. Data are expressed in mean ± SE (n = 5) and comparison was made between control groups and treated groups using one way ANOVA with Student *t*-test ($^{**}p < 0.01$ and $^{***}p < 0.001$).

LD_{50} values typically greater than 2000 mg/kg body weight in mice and rats [65].

The application of phytochemicals in cancer prevention and therapy effectively reduces the risk of cancer in humans [66]. The epidemiological studies have demonstrated that terpenoids play a pivotal role in preventing the progression of cancer and significantly suppress the tumor cells [67,68]. Terpenoids (menthol and limonene) are considered as the most effective transdermal penetration enhancers and ease the accessibility of other drugs [69]. Due to the hydrophobic nature of terpenes (Menthol: Log p-value of 3.4), they interact with the lipids moiety of the plasma membrane and enhances the drug permeation through the skin [70,71]. Therefore, neomenthol, with its hydrophobic and lipophilic character, is successfully establishing an interaction with the membrane lipids and disrupts the cellular environment which might leads to A431 cells death. Furthermore, the modulation of

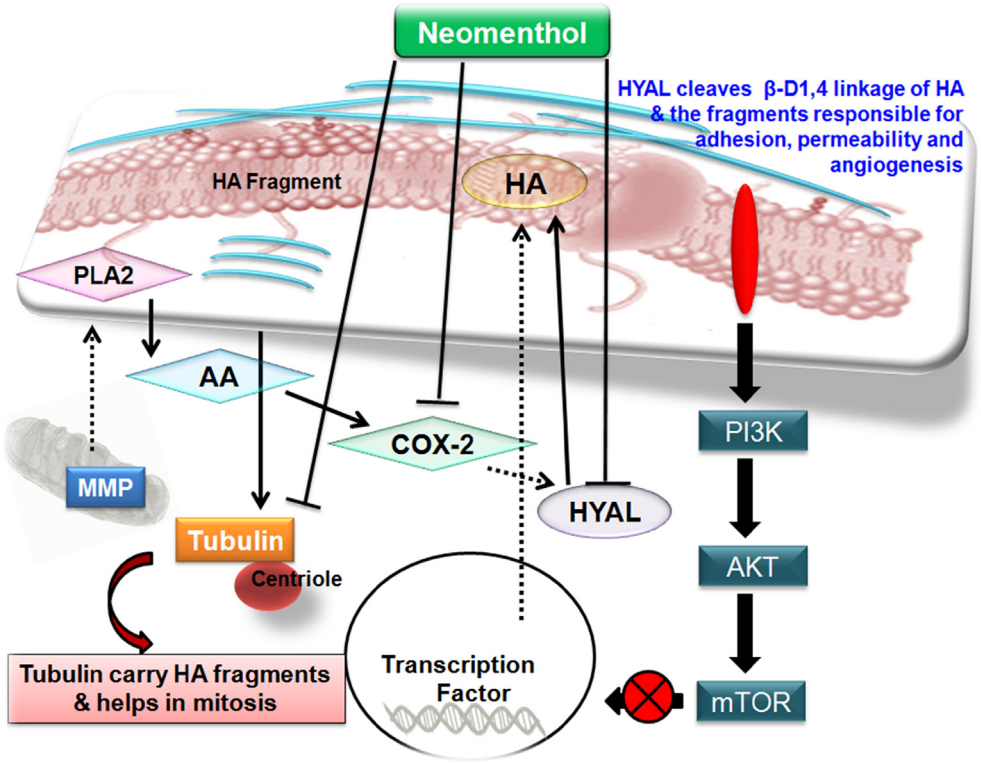

Fig. 7. Summary of neomenthol in modulating the expression of initiation (PI3K, AKT, mTOR, Tubulin), promotion (HDAC-6, COX-2), and progression (hyaluronidase) phase biomarkers in A431 cells. In cancer cells, upside (↑) arrow showed higher expression of biomarkers and downside arrow (↓) depicts the decrease of biomarker expression by neomenthol.

hyaluronidase activity by neomenthol affects the HA content, which is significantly employed in the development of dermal and transdermal drug delivery systems and regulation of pro-inflammatory signaling in tumor promotion [72,73].

Neomenthol also inhibits the polymerization of tubulin due to which dynamic property of A431 cells was disturbed, which might also be leading to apoptosis. The cell cycle analysis further confirms the apoptosis by showing the cell arrest at the G2/M phase, followed by an increase in the number of sub-diploid cells. Additionally, the reduction in mitochondrial membrane potential and an increase in ROS supported the antiproliferation of A431 cells. Long-term exposure of cells to menthol increases toxicity and the problem of a fibroblast-like morphology, loss of cell-to-cell junctions, internalization of E-cadherin, increased motility, and upregulation of other EMT markers was observed [74]. Surprisingly, compared to menthol, neomenthol was found non- toxic, though FDA has approved the use of 16% of menthol in OTC preparation for external application [70]. The duke database revealed that the LD_{50} of menthol is 700 to 3300mg/kg [Phytochem.nal.usda.gov/phytochem/chemicals/show/12107] whereas neomenthol is 4000 mg/kg [https://chem.nlm.nih.gov/chemidplus/rn/3623–51-6]. This data strongly supports our results wherein no toxicity of neomenthol was found upto 1000 mg/kg bw in mice followed by the non-deviation of Lipinski rule of five and erythrocytes permeability. Considering the data of the present study, neomenthol showed chemopreventive effect in cell-free and cell-based molecular target analysis. A schematic representation of the hypothesis is shown in Fig. 7.

Conclusion

Neomenthol modulates the expression of biomarkers involves in initiation (PI3K, AKT, mTOR, tubulin), promotion (HDAC-6, COX-2), and progression (hyaluronidase) stages of carcinogenesis. Neomenthol retarded the growth of A431 cells by significantly modulating the expression of hyaluronidase, which cannot degrade HA, and the interference with hyalurondase structure results in the apoptos is of the cell. It correlates well with the molecular docking interaction studies and real-time gene expression analysis. Neomenthol also inhibits the polymerization of tubulin and revealed a pleiotropic mode of action by modulating different biomarkers, which in turn regulate the unsynchronized pathways/biomarkers in cancer cells. As neomenthol is 1-epimer of menthol, its biological activity is reported similar to that of menthol but astonishingly non-toxic.

Compliance with Ethics Requirements

All Institutional and National Guidelines for the care and use of animals were followed.

Declaration of Competing Interest

The authors declare that they have no known competing financial interests or personal relationships that could have appeared to influence the work reported in this paper.

Acknowledgment

We are grateful to the Director, CSIR-Central Institute of Medicinal and Aromatic Plants, Lucknow, for providing necessary facilities to carry out the research work under CSIR-Aroma Mission (HCP 007) project. KF & NM acknowledges the Council of Scientific & Industrial Research (CSIR), New Delhi, for Senior Research Fellowship. ZAW thanks SERB, New Delhi, for National Post-Doctoral Fellowship. We are thankful to Dr. J. Sarkar, CSIR-CDRI, Lucknow, for providing FaDU cell line.

Appendix A. Supplementary material

Supplementary data to this article can be found online at https://doi.org/10.1016/j.jare.2021.06.003.

References

[1] Rayan A, Raiyn J, Falah M. Nature is the best source of anticancer drugs: Indexing natural products for their anticancer bioactivity. PLoS ONE 2017;12:. doi: https://doi.org/10.1371/journal.pone.0187925e0187925.

[2] Eccles R. Menthol and Related Cooling Compounds. J Pharm Pharmacol 1994;46:618–30. doi: https://doi.org/10.1111/j.2042-7158.1994.tb03871.x.

[3] McKemy DD, Neuhausser WM, Julius D. Identification of a cold receptor reveals a general role for TRP channels in thermosensation. Nature 2002;416:52.

[4] Peier AM, Reeve AJ, Andersson DA, Moqrich A, Earley TJ, Hergarden AC, et al. A heat-sensitive TRP channel expressed in keratinocytes. Science 2002;296:2046–9.

[5] Terpenes Breitmaier E. Importance, general structure, and biosynthesis. Terpenes: Flavors, Fragrances, Pharmaca. Pheromones 2006:1–9. doi: https://doi.org/10.1002/9783527609949.

[6] Bernhardt G, Biersack B, Bollwein S, Schobert R, Zoldakova M. Terpene Conjugates of Diaminedichloridoplatinum (II) Complexes: Antiproliferative Effects in HL-60 Leukemia, 518A2 Melanoma, and HT-29 Colon Cancer Cells. Chem Biodivers 2008;5:1645–59.

[7] Weecharangsan W, Sithithaworn W, Siripong P. Cytotoxic activity of essential oils of MenthaSps. On human carcinoma cells. J Health Res 2014;28:9–12.

[8] Kuttan G, Pratheeshkumar P, Manu KA, Kuttan R. Inhibition of tumor progression by naturally occurring terpenoids. Pharma Bio 2011;49:995–1007. doi: https://doi.org/10.3109/13880209.2011.559476.

[9] Barthelman M, Chen W, Gensler HL, Huang C, Dong Z, Bowden GT. Inhibitory effects of perillyl alcohol on UVB-induced murine skin cancer and AP-1 transactivation. Cancer Res 1998;58:711–6.

[10] Haag JD, Gould MN. Mammary carcinoma regression induced by perillyl alcohol, a hydroxylated analog of limonene. Cancer Chemother Pharmacol 1994;34:477–83.

[11] Wattenberg LW, Coccia JB. Inhibition of 4-(methylnitrosamino)-1-(3-pyridyl)-1-butanone carcinogenesis in mice by D-limonene and citrus fruit oils. Carcinogenesis 1991;12:115–7.

[12] Crowell PL. Prevention and therapy of cancer by dietary monoterpenes. Nutr J 1999;129:775S–8S.

[13] Mosmann T. Rapid colorimetric assay for cellular growth and survival: application to proliferation and cytotoxicity assays. J Immunol Methods 1983;65:55–63.

[14] Babich H, Borenfreund E. Cytotoxicity of T-2 toxin and its metabolites determined with the neutral red cell viability assay. Appl Environ Microbiol 1991;57:2101–3.

[15] Shekan P, Storeng R, Scudiero D, Monks A, McMahon J, Vistica D, et al. New colorimetric cytotoxicity assay for anticancer-drug screening. J Natl Cancer Inst 1990;82:1107–12.

[16] Kulmacz RJ, Lands WE. Requirements for hydroperoxide by the cyclooxygenase and peroxidase activities of prostaglandin H synthase. Prostaglandins 1983;25:531–40.

[17] Cho YS, Kim HS, Kim CH, Cheon HG. Application of the ferrous oxidation–xylenol orange assay for the screening of 5-lipoxygenase inhibitors. AnalBiochem 2006;351:62–8.

[18] Hillcoat BL, Nixon PF, Blakley RL. Effect of substrate decomposition on the spectrophotometric assay of dihydrofolatereductase. AnalBiochem 1967;21:178–89.

[19] Dorfman A, Ott ML. A turbidimetric method for the assay of hyaluronidase. J BiolChem 1948;172:367–75.

[20] Luqman S, Masood N, Srivastava S, Dubey V. A Modified Spectrophotometric and Methodical Approach to Find Novel Inhibitors of Ornithine Decarboxylase Enzyme: A Path through the Maze. Protoc Exch 2013;10:1–25. doi: https://doi.org/10.1038/protex.2013.045.

[21] Smith R, Turk V. Cathepsin D: rapid isolation by affinity chromatography on haemoglobin-agarose resin. Eur J Biochem 1974;48:245–54.

[22] Singh S, Dubey V, Singh DK, Fatima K, Ahmad A, Luqman S. Antiproliferative and antimicrobial efficacy of the compounds isolated from the roots ofOenotherabiennis L. J Pharm Pharmacol 2017;69:1230–43.

[23] Morris GM, Goodsell DS, Halliday RS, Huey R, Hart WE, Belew RK, et al. Automated docking using a Lamarckian genetic algorithm and an empirical binding free energy function. J ComputChem 1998;19:1639–62.

[24] Seniya C, Khan GJ, Uchadia K. Identification of potential herbal inhibitor of acetylcholinesterase associated Alzheimer's disorders using molecular docking and molecular dynamics simulation. Biochem Res Int 2014;2014:. doi: https://doi.org/10.1155/2014/705451705451.

[25] Bustin SA, Benes V, Garson JA, Hellemans J, Huggett J, Kubista M, et al. The MIQE guidelines: minimum information for publication of quantitative real-time PCR experiments. ClinChem 2009;55:611–22.

[26] Singh A, Fatima K, Singh A, Behl A, Mintoo MJ, Hasanain M, et al. Anticancer activity and toxicity profiles of 2-benzylidene indanone lead molecule. Eur J Pharm Sci 2015;76:57–67.

[27] Khwaja S, Fatima K, Hasanain M, Behera C, Kour A, Singh A, et al. Antiproliferative efficacy of curcumin mimics through microtubule destabilization. Eur J Med Chem 2018;151:51–61.

[28] Braicu C, Pilecki V, Balacescu O, Irimie A, BerindanNeagoe I. The relationships between biological activities and structure of flavan-3-ols. Int J Mol Sci 2011;12:9342–53.

[29] Wani ZA, Guru SK, Rao AS, Sharma S, Mahajan G, Behl A, et al. A novel quinazolinonechalcone derivative induces mitochondrial dependent apoptosis and inhibits PI3K/Akt/mTOR signaling pathway in human colon cancer HCT-116 cells. Food ChemToxicol 2016;87:1–11.

[30] Rajkapoor B, Jayakar B, Murugesh N. Antitumor activity of Indigoferaaspalathoides on Ehrlich ascites carcinoma in mice. Indian J Pharmacol 2004;36:38.

[31] Luqman S, Rizvi SI. Protection of lipid peroxidation and carbonyl formation in proteins by capsaicin in human erythrocytes subjected to oxidative stress. Phytother Res 2006;20:303–6.

[32] Singh A, Fatima K, Srivastava A, Khwaja S, Priya D, Singh A, et al. Anticancer activity of gallic acid template-based benzylideneindanone derivative as microtubule destabilizer. Chem Biol Drug Des 2016;88:625–34.

[33] Yamamura H, Ugawa S, Ueda T, Morita A, Shimada S. TRPM8 activation suppresses cellular viability in human melanoma. Am J Physiol Cell Physiol 2008;295:C296–301.

[34] Kim SH, Nam JH, Park EJ, Kim BJ, Kim SJ, So I, et al. menthol regulates TRPM8-independent processes in PC-3 prostate cancer cells. Biochim Biophys Acta (BBA)-Mol Basis Dis 2009;1792:33–8.

[35] Wang Y, Wang X, Yang Z, Zhu G, Chen D, Meng Z. Menthol inhibits the proliferation and motility of prostate cancer DU145 cells. Pathol Oncol Res 2012;18:903–10.

[36] Liu Z, Shen C, Tao Y, Wang S, Wei Z, Cao Y, et al. Chemopreventive efficacy of menthol on carcinogen-induced cutaneous carcinoma through inhibition of inflammation and oxidative stress in mice. Food ChemToxicol 2015;82:12–8.

[37] Negi AS, Gautam Y, Alam S, Chanda D, Luqman S, Sarkar J, et al. Natural antitubulin agents: Importance of 3, 4, 5-trimethoxyphenyl fragment. Bioorg Med Chem 2015;23:373–89.

[38] Rioja A, Pizzey AR, Marson CM, Thomas NSB. Preferential induction of apoptosis of leukaemic cells by farnesol. FEBS Lett 2000;467:291–5.

[39] Harris RC, Zhang M-Z, Cheng H-F. Cyclooxygenase-2 and the renal renin–angiotensin system. Acta Physiol Scand 2004;181:543–7.

[40] Wiese FW, Thompson PA, Kadlubar FF. Carcinogen substrate specificity of human COX-1 and COX-2. Carcinogenesis 2001;22:5–10.

[41] Zarghi A, Arfaei S. Selective COX-2 inhibitors: a review of their structure-activity relationships. Iran J Pharma Res 2011;10:655.

[42] Ringleb J, Strack E, Angioni C, Geisslinger G, Steinhilber D, Weigert A, et al. Apoptotic cancer cells suppress 5-lipoxygenase in tumor-associated macrophages. J Immunol 2018;200:857–68.

[43] Juergens UR, Stöber M, Vetter H. The anti-inflammatory activity of L-menthol compared to mint oil in human monocytes in vitro: a novel perspective for its therapeutic use in inflammatory diseases. Eur J Med Res 1998;3:539–45.

[44] Kamatou GP, Vermaak I, Viljoen AM, Lawrence BM. Menthol: a simple monoterpene with remarkable biological properties. Phytochemistry 2013;96:15–25.

[45] Dubey V, Luqman S. Cathepsin D as a Promising Target for the Discovery of Novel Anticancer Agents. Curr Cancer Drug Targets 2017;17:404–22.

[46] Fronza M, Caetano GF, Leite MN, Bitencourt CS, Paula-Silva FW, Andrade TA, et al. Hyaluronidase modulates inflammatory response and accelerates the cutaneous wound healing. PLoS ONE 2014;9:. doi: https://doi.org/10.1371/journal.pone.0112297e112297.

[47] Heller JS, Fong WF, Canellakis ES. Induction of a protein inhibitor to ornithine decarboxylase by the end products of its reaction. Proc Natl Acad Sci 1976;73:1858–62.

[48] Arumugam A, Weng Z, Talwelkar SS, Chaudhary SC, Kopelovich L, Elmets CA, et al. Inhibiting cycloxygenase and ornithine decarboxylase by diclofenac and alpha-difluoromethylornithine blocks cutaneous SCCs by targeting Akt-ERK axis. PLoS ONE 2013;8:. doi: https://doi.org/10.1371/journal.pone.0080076e80076.

[49] Carnesecchi S, Schneider Y, Ceraline J, Duranton B, Gosse F, Seiler N, et al. Geraniol, a component of plant essential oils, inhibits growth and polyamine biosynthesis in human colon cancer cells. J Pharmacol Exp Ther 2001;298:197–200.

[50] Majumdar ID, Devanabanda A, Fox B, Schwartzman J, Cong H, PorcoJr JA, et al. Synthetic cyclohexenylchalcone natural products possess cytotoxic activities against prostate cancer cells and inhibit cysteine cathepsins in vitro. Biochem Bioph Res Comm 2011;416:397–402.

[51] Avenoso A, D'Ascola A, Scuruchi M, Mandraffino G, Calatroni A, Saitta A, et al. Hyaluronan in the experimental injury of the cartilage: biochemical action and protective effects. Inflamm Res 2018;67:5–20. doi: https://doi.org/10.1007/s00011-017-1084-9.

[52] Serra M, Reverter-Branchat G, Maurici D, Benini S, Shen J-N, Chano T, et al. Analysis of dihydrofolatereductase and reduced folate carrier gene status in relation to methotrexate resistance in osteosarcoma cells. Ann Oncol 2004;15:151–60.

[53] Rao AS, Tapale SR. A study on dihydrofolatereductase and its inhibitors: a review. Int J Pharm Sci Res 2013;4:2535.

[54] Faridi U, Sisodia BS, Shukla AK, Shukla RK, Darokar MP, Dwivedi UN, et al. Proteomics indicates modulation of tubulin polymerization by L-menthol

inhibiting human epithelial colorectal adenocarcinoma cell proliferation. Proteomics 2011;11:2115–9.
[55] Wang J, Yi J. Cancer cell killing via ROS: to increase or decrease, that is the question. Cancer BiolTher 2008;7:1875–84.
[56] Chueca B, Pagán R, García-Gonzalo D. Oxygenated monoterpenescitral and carvacrol cause oxidative damage in Escherichia coli without the involvement of tricarboxylic acid cycle and Fenton reaction. Int J Food Microbiol 2014;189:126–31.
[57] Manning BD, Toker A. AKT/PKB signaling: navigating the network. Cell 2017;169:381–405.
[58] Aldana-Masangkay GI, Rodriguez-Gonzalez A, Lin T, Ikeda AK, Hsieh Y-T, Kim Y-M, et al. Tubacin suppresses proliferation and induces apoptosis of acute lymphoblastic leukemia cells. Leukemia Lymphoma 2011;52:1544–55.
[59] Jia S-S, Xi G-P, Zhang M, Chen Y-B, Lei B, Dong X-S, et al. induction of apoptosis by D-limonene is mediated by inactivation of Akt in LS174T human colon cancer cells. Oncol Rep 2013;29:349–54.
[60] Mishra S, Tamta AK, Sarikhani M, Desingu PA, Kizkekra SM, Pandit AS, et al. Subcutaneous Ehrlich Ascites Carcinoma mice model for studying cancer-induced cardiomyopathy. Sci Rep 2018;8:5599.
[61] McAtee CO, Barycki JJ, Simpson MA. Emerging roles for hyaluronidase in cancer metastasis and therapy. Adv Cancer Res 2014;123:1–34.
[62] Lokeshwar VB, Rubinowicz D, Schroeder GL, Forgacs E, Minna JD, Block NL, et al. Stromal and Epithelial Expression of Tumor Markers Hyaluronic Acid and HYAL1 Hyaluronidase in Prostate Cancer. J Biol Chem 2001;276:11922–32.
[63] Kohi S, Sato N, Koga A, Hirata K, Harunari E, Igarashi Y. Hyaluromycin, a Novel Hyaluronidase Inhibitor, Attenuates Pancreatic Cancer Cell Migration and Proliferation. J Oncol 2016;2016:9063087. doi: https://doi.org/10.1155/2016/9063087.
[64] Bhal SK. LogP—Making Sense of the Value. www.acdlabs.com/logp/ Advanced Chemistry Development, Inc., Toronto, ON, Canada. 2011; pp 1-4.
[65] Oz M, El Nebrisi EG, Yang K-HS, Howarth FC, Al Kury LT. Cellular and molecular targets of menthol actions. Front Pharmacol 2017;8:472.
[66] Greenlee H. Natural products for cancer prevention. Semin Oncol Nurs 2012;28:29–44.
[67] Huang M, Lu J-J, Huang M-Q, Bao J-L, Chen X-P, Wang Y-T. Terpenoids: natural products for cancer therapy. Expert Opin Invest Drugs 2012;21:1801–18.
[68] Upadhyay S, Dixit M. Role of polyphenols and other phytochemicals on molecular signaling. Oxid Med Cell Longev 2015;2015:. doi: https://doi.org/10.1155/2015/504253504253.
[69] Patel T, Ishiuji Y, Yosipovitch G. Menthol: a refreshing look at this ancient compound. J Am Acad Dermatol 2007;57:873–8.
[70] A.del V. Turina M.V. Nolan J.A. Zygadlo M.A. Perillo Natural terpenes: self-assembly and membrane partitioning Biophy Chem 122 2006 101 113
[71] Vaddi HK, Ho PC, Chan SY. Terpenes in propylene glycol as skin-penetration enhancers: Permeation and partition of haloperidol, fourier transform infrared spectroscopy, and differential scanning calorimetry. J Pharm Sci 2002;91:1639–51.
[72] Toole BP. Hyaluronan: from extracellular glue to pericellular cue. Nat Rev Cancer 2004;4:528.
[73] Spicer AP, Tien JY. Hyaluronan and morphogenesis. Birth Defects Res Part C: Embryo Today: Rev 2004;72:89–108.
[74] Zahedi A, Phandthong R, Chaili A, Remark G, Talbot P. Epithelial-to-mesenchymal transition of A549 lung cancer cells exposed to electronic cigarettes. Lung Can 2018;122:224–33.